

Mathematical Statistics
Stockholm University

A Statistical Analysis of Heart Tissue Perforations

Kristoffer Spricer

Examensarbete 2009:8

Postal address:

Mathematical Statistics
Dept. of Mathematics
Stockholm University
SE-106 91 Stockholm
Sweden

Internet:

<http://www.math.su.se/matstat>



Mathematical Statistics
Stockholm University
Examensarbete **2009:8**,
<http://www.math.su.se/matstat>

A Statistical Analysis of Heart Tissue Perforations

Kristoffer Spricer*

September 2009

Abstract

When implanting the lead, the electrical connector that leads the electrical impulses between the heart and the pacemaker, a severe complication can occur. On rare occasions, the tip of the lead goes all the way through the heart wall, perforating it fully. It is critical to understand what factors control these perforations so that they can be avoided. This thesis focuses on performing a full statistical analysis of perforation test data on porcine heart tissue collected in 2007 by Robin Hosselton, with some key questions in mind. Specifically it is shown that a good model for the perforation data is the log-normal distribution. This means that a logarithmic transformation of the data is required when performing a statistical analysis of this type of data. We also show that the relationship between the perforation force and the lead tip diameter can be modeled using a linear function. Some additional analyses show that the tissue is not homogeneous, i.e. that it has stronger and weaker areas. Included is the definition of a correlation coefficient that can be used to characterize the tissue and also a demonstration of the use of a graphical visualization method. These findings have implications both on how to perform perforation tests, but also on the modeling of soft biological tissue. Any proper model should show properties similar to those found in experiments such as the one performed by Robin Hosselton, and this statistical analysis makes it possible to incorporate the findings in useful perforation models.

*Postal address: Mathematical Statistics, Stockholm University, SE-106 91, Sweden.
E-mail: KSpricer@sjm.com. Supervisor: Tom Britton.

A Statistical Analysis of Heart Tissue Perforations

Kristoffer Spricer

September 2009

Abstract

When implanting the *lead*, the electrical connector that leads the electrical impulses between the heart and the pacemaker, a severe complication can occur. On rare occasions, the tip of the lead goes all the way through the heart wall, perforating it fully. It is critical to understand what factors control these perforations so that they can be avoided. In 2007, Robin Hosselton carried out a largely experimental work, performing about 1400 perforations of porcine right ventricular cardiac tissue with the intention to understand the mechanisms of heart wall perforation better.

This thesis focuses on performing a full statistical analysis of the extensive data material with some key questions in mind. Specifically we show that a good model for the perforation data is the log-normal distribution. This finding has important implications for everyone performing this type of perforation tests, as it requires a logarithmic transformation of the data in order to draw the correct conclusions from experiments. We also show that the relationship between the perforation force and the lead tip diameter can be modeled using a linear function. This has implications on using the tip pressure as a limiting value for lead design. A better parameter would be the force divided by the diameter, as this quotient does not so strongly depend on the diameter of the lead tip. Some additional analyses show that the tissue is not homogeneous, i.e. that it has stronger and weaker areas. Included is the definition of a correlation coefficient that can be used to characterize the tissue and also a demonstration of the use of a graphical visualization method.

These findings have implications both on how to perform perforation tests, but also on the modeling of soft biological tissue. Any proper model should show properties similar to those found in experiments such as the one performed by Robin Hosselton, and this statistical analysis makes it possible to incorporate the findings in useful perforation models.

Acknowledgements

I would like to thank Tom Britton, my supervisor at Stockholm University, for suggesting statistical methods to be used for the analysis of the perforation data and for good ideas on the content and layout of the thesis. I would also like to thank Robin Hosselton who collected all the data analyzed here and the KTH Royal Institute of Technology, especially Christian Gasser, for allowing me to use the full data set in this extended statistical analysis.

At St. Jude Medical, I would like to thank my manager Johan Sköld for supporting my work on the thesis, Lennart Lundström for ideas on what should be included in it and finally Marcus Helgesson for important discussions regarding the original experiments and the results of the statistical analysis.

Contents

1	Introduction	4
2	Background	5
2.1	The Pacemaker and the ICD	5
2.2	Heart Physiology and Pacemaker/ICD Implantation	7
2.3	Perforation Risk	8
2.4	Performing Perforation Tests	9
2.5	Use of Porcine Tissue	11
2.6	Terminology and Abbreviations	12
3	Key Questions	13
4	The Performed Tests	14
4.1	Perforation Tests	14
4.2	Tissue Samples	14
4.3	Punch Samples	14
4.4	Test Equipment	15
5	The Data Material	16
5.1	Overview	16
5.2	Order of Perforation and Randomization	17
5.3	Extracted Parameters	19
5.4	Software for Extraction of Parameters	19
5.5	Identification of the Point of First Damage	19
6	Statistical Analysis	21
6.1	Assessment of the Homogeneity of the Porcine Tissue	21
6.2	Does the Tissue Exhibit any Aging Effect?	29
6.3	The Effect of the Helix	36
6.4	Statistical Analysis of Solid and Tubular Punches	40
6.5	Discussion Regarding the Logarithmic Transformation	51
7	Summary and Conclusions	53
7.1	Answers to Key Questions	53
7.2	Final Conclusions	54
7.3	Recommendations for Future Work	54
	References	56

1 Introduction

The pacemaker and the ICD (Implantable Cardioverter-Defibrillator) can save lives and improve the quality of life for heart patients all over the world. However, when implanting the lead, the electrical connector that leads the electrical impulses between the heart and the pacemaker, there is a rare, but severe complication that may occur. This is when the tip of the lead goes all the way through the heart wall, instead of attaching to the surface of the heart as intended. Leads are designed with focus to reduce the risk of such heart wall perforations and physicians use procedures intended to avoid the risk. The knowledge to why these perforations occur is still very limited.

In 2007, Robin Hosselton performed a novel and extensive experimental work as part of his Master Thesis [2]. He performed about 1400 quasi-static perforations on 14 porcine cardiac tissue samples with the intention of investigating how the perforation force depended on such properties as the diameter and the shape of the tip of the lead. His thesis from 2008 included the analysis of more than 1000 perforations from 12 tissue samples. While being extensive the work did not include a full statistical analysis of the data material. The intention of this thesis is to remedy this and to use statistical methods to get as much information out of the available data as possible. Extra important is to see if the results are statistically significant. For the reader who is new to the subject Chapter 2 is recommended for a comprehensive background on pacemakers, implantation and heart wall perforations, and in Chapters 4 and 5 the performed perforation tests and the available data material are presented in more detail.

Before the analysis begins, we define a set of key questions in Chapter 3. These are questions of both practical and statistical importance. Some questions are in line with the intention of Hosselton's original work, while answers to other questions are required to be able to utilize the data material fully. Examples of key questions are if the tissue ages during the time it takes to perform the tests, if the tissue is homogeneous or has stronger and weaker areas, and how the perforation force is distributed. This later question has strong bearing on any statistical modeling of heart wall perforation, while the first questions could affect the perforation test design and the mechanical modeling of tissue strength.

Specifically, in Section 6.2 we will see that the tissue does not exhibit any aging during the testing. This allows us to use all the data available in the full analysis, even though the experiments were not fully randomized in terms of perforation order, and we see that the log-normal distribution can be used to model the perforation force data with good results (Section 6.5). This important finding has implications for everyone performing this type of perforation tests. It shows that it is not enough to use the mean and the standard deviation for the original force data when drawing conclusions about the results of experiments, but that a logarithmic transformation of the data is required.

Conclusions regarding how the perforation force depends on the diameter and the shape of the tip of the lead can be found in Sections 6.3 and 6.4. Here we see that using the pressure as a limiting factor for leads (as is common in lead development) is probably not the best choice as the pressure required to perforate the tissue is not independent of the lead diameter. A better parameter is the force divided by the diameter, as this quotient does not so strongly depend on the diameter of the lead tip.

As a bonus, we investigate a new way of characterizing the homogeneity of the tissue sample by defining a correlation coefficient for the tissue in a way that is analogous to Pearson's sample correlation coefficient. To this method we add a graphical force mapping method so that the force distribution on the tissue can be viewed in 3D for easier inspection. This allows for visual identification of abnormal areas on the tissue.

At the end of the thesis, a complete list of answers to the key questions can be found and also some proposals for future work (Chapter 7).

2 Background

In order to understand the experiments, the analysis of them and the conclusions some background information is needed. This Chapter gives a brief introduction to the pacemaker/ICD system (Section 2.1), heart physiology and implantation (Section 2.2), heart wall perforations (Section 2.3) and perforation testing (Sections 2.4 and 2.5). There is also a list of terminology and abbreviations to aid the reader (Section 2.6).

2.1 The Pacemaker and the ICD

The pacemaker and the ICD are both devices that are used when the patient's heart is not functioning normally; however, they are aimed at different heart conditions.

- The **pacemaker** takes on the function of maintaining a normal, even heart rhythm if the patient's heart beats too slowly or not at all. It does so by supplying a low voltage pulse if it does not detect a normally paced heartbeat. The pulse triggers the heart into a normal heartbeat.
- The **ICD** is aimed at preventing or breaking a too fast, often irregular heart rhythm, such as a flutter or a fibrillation in the right ventricle. These later are both conditions that can either reduce the hearts capacity to pump blood or prevent the blood flow completely. The latter condition is very dangerous and needs immediate treatment. In response to detecting such a condition, the ICD is designed to emit one or more high voltage pulses. The high voltage pulse "resets" the heart to normal operation and allows it to resume its normal rhythm.

In order for the pacemaker or ICD (from here on called *the device*) to be able to treat the heart condition they need to be connected electrically to the heart. Since the device is too big to be implanted in the heart itself, it is instead connected to the heart using an electrical wire. This type of wire is called a lead (see Figure 2.1).

At the *proximal* end of the lead (the end closest to the device) is a connector that connects securely to the device. At the *distal* end (the end furthest from the device), there is an electrode that is implanted in the heart and connects electrically to the heart. The tip may also have tines, fins or a helix that aids in attaching the lead to the heart wall.

Two types of leads are used (see Figure 2.2):

Passive leads:

The lead is held in place by fins or tines that attach to the inner structure of the heart. This type of lead is mechanically simple, and usually has a soft, flexible tip.

Active leads:

The lead is attached using a helix that is extended from the header at the distal end of the lead. This type of lead is mechanically more complex as it needs to house the helix mechanism, and a portion (10-20 mm) of the tip is usually rigid and cannot bend.

More information on the pacemaker system can be found in [3].

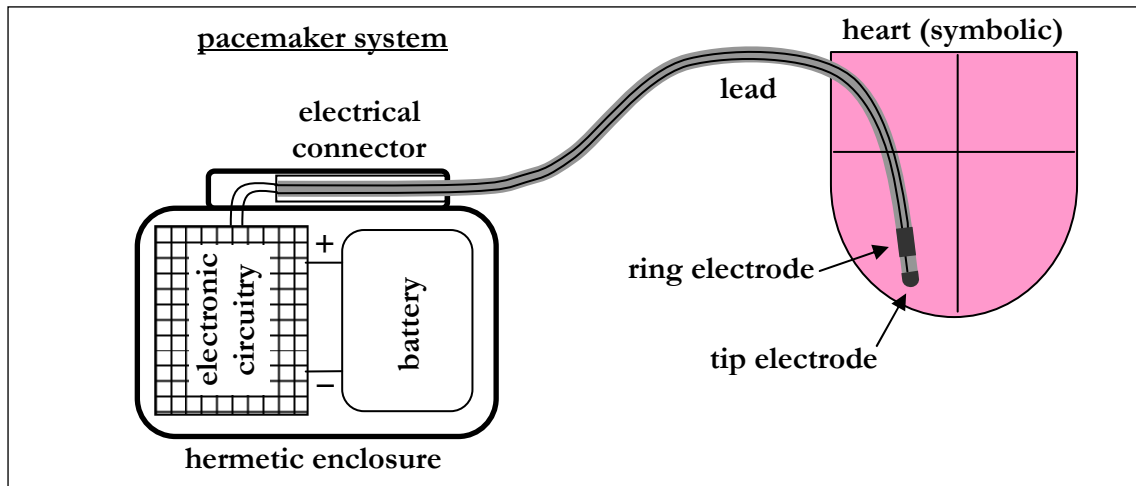


Figure 2.1: A schematic overview of the simplest pacemaker system with only one lead. The pacemaker contains a battery and electronic circuitry, and is connected electrically to the heart via the lead.

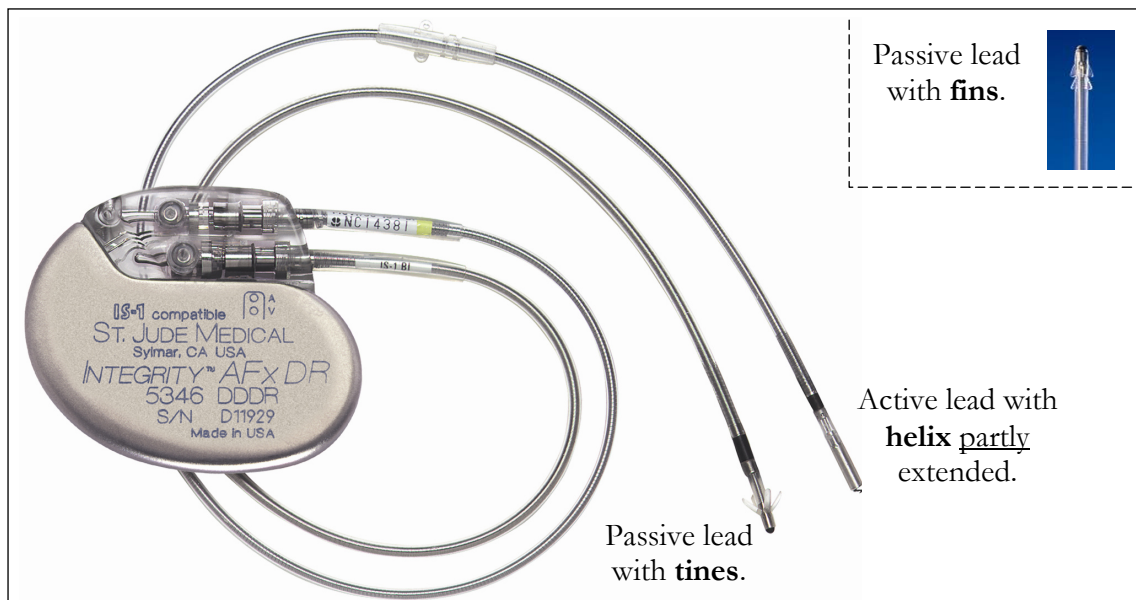


Figure 2.2: The figure shows a St. Jude Medical pacemaker with two leads attached; one with passive and one with active fixation. Active fixation using a helix requires the physician to extend the helix manually into the heart wall during the implantation. The passive lead often uses tines or fins to attach itself to the tissue inside the heart.

2.2 Heart Physiology and Pacemaker/ICD Implantation

An overview of the human heart can be seen in the Figure 2.3.

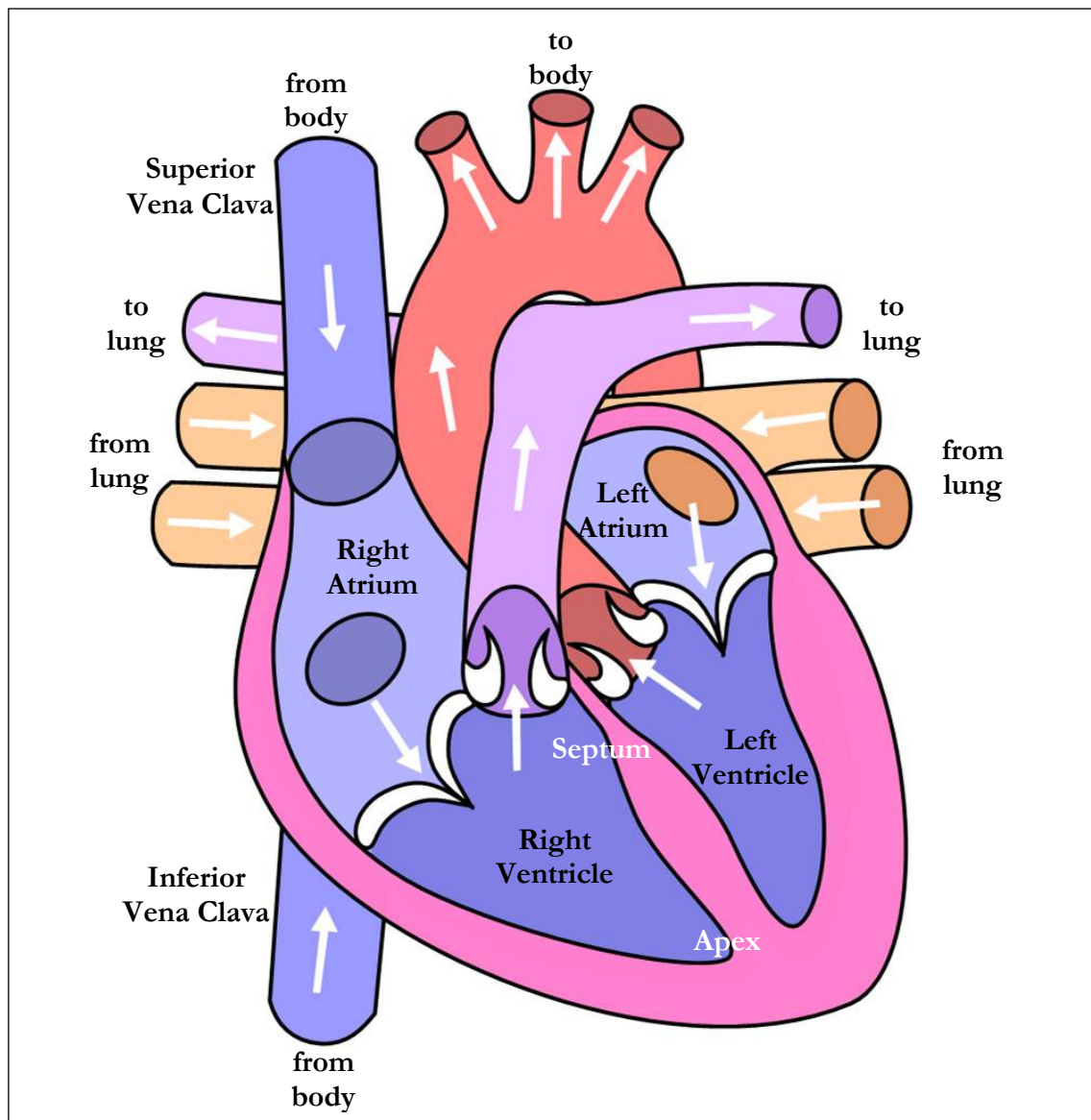


Figure 2.3: Overview of the human heart¹. White arrows indicated direction of blood flow. The most common implantation of pacemaker and ICD leads is through Superior Vena Clava into the right atrium or right ventricle. Common implantation sites are the ventricular apex or the ventricular upper septum wall (white text in the figure).

When a lead is implanted in the heart this is usually done through Superior Vena Clava. Most leads are implanted in the right atrium or the right ventricle. The procedure is performed under local anesthesia and typically takes less than one hour. Normally only one

¹ The figure has been adapted from Wikipedia Commons: 'Diagram_of_the_human_heart_(cropped).svg'.

incision is made both for the entry into the vein and for the placement of the device. The patient can leave the hospital the same day.

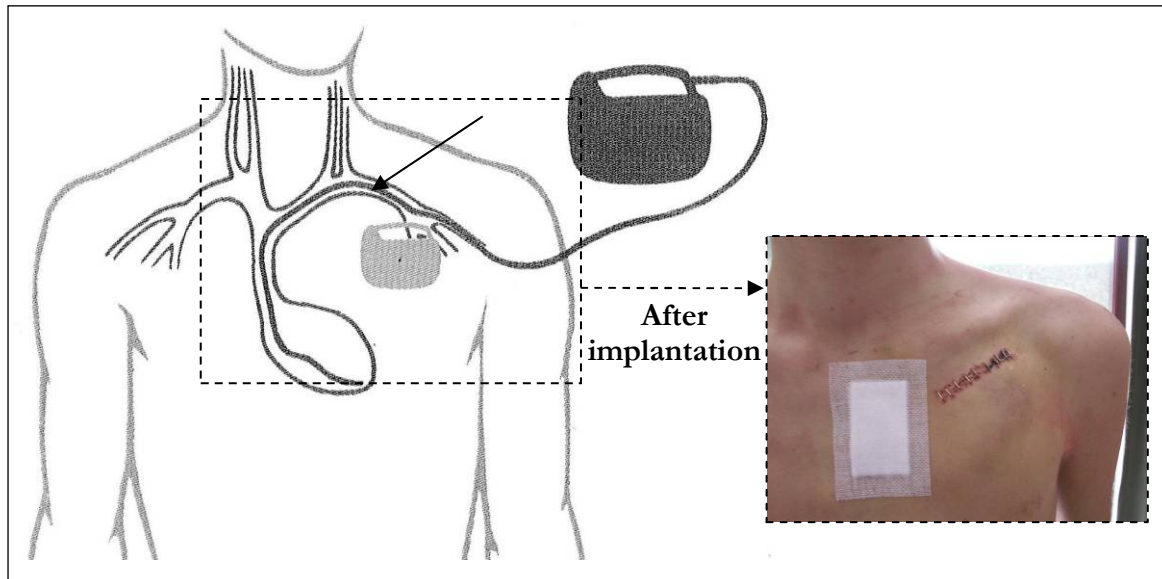


Figure 2.4: The left figure² shows where the device is placed and how the lead enters the heart through the vein. The right photograph³ shows the wound left after the implantation. The location of the pacemaker is just below the wound, just under the breast muscle.

More information on heart physiology and implantation can be found in [3].

2.3 Perforation Risk

For both passive and active leads, it is important that the lead tip has firm contact with the heart wall after the implantation and that it does not move. For an active lead, the helix needs to be fully attached to the heart wall (see Figure 2.5). If the helix is not fully attached, the lead may be dislodged later and the pacemaker will fail to stimulate the heart. Therefore, some force must be used during helix extension, but if too much force is applied, the lead may penetrate the heart wall and the tip will enter the myocardium. Continued application of force, or increased force level may eventually push the lead through the entire heart wall, resulting in a full perforation possibly even collapsing the lungs - a dangerous condition that requires immediate medical treatment.

During implantation the physician cannot measure the strength of the tissue at the selected implantation site. Therefore, the risk of perforation is higher when he by chance chooses a weak position rather than a strong one. When analyzing tissue strength, extra attention should be given to the weaker parts of the tissue, as they will contribute more to the perforation risk than will the stronger parts.

² The figure is copied from [3], page 171.

³ The photo is taken from Wikipedia Commons: 'Pacemaker_Wound.jpg'.

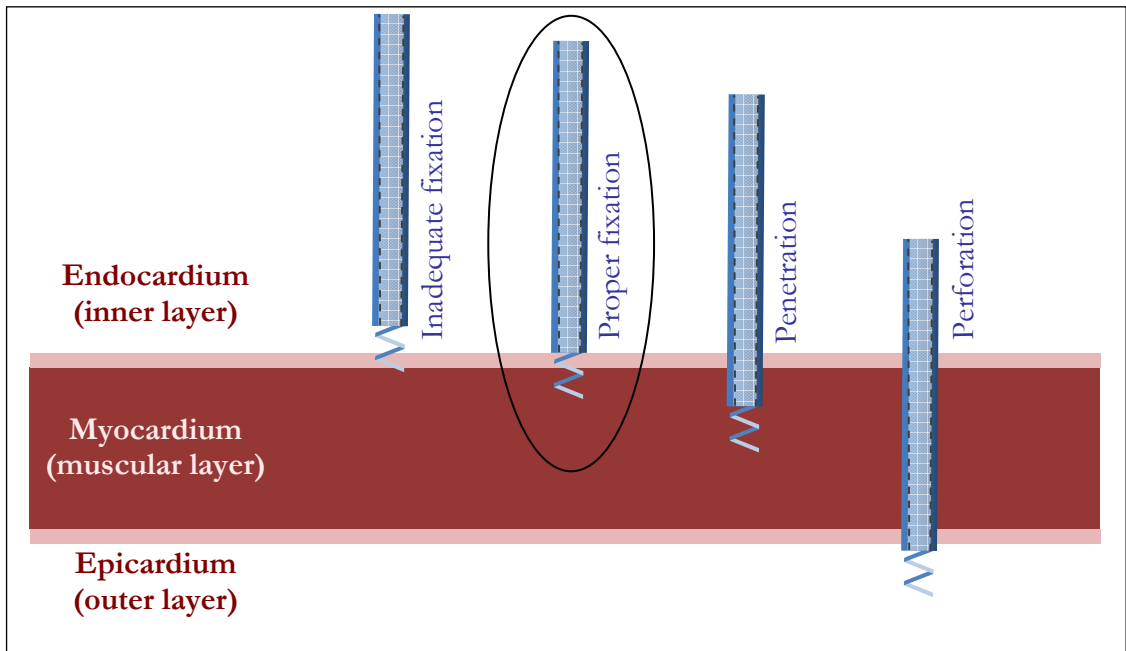


Figure 2.5: The figure shows the heart wall with the three main layers: the inner endocardium, the myocardium and the outer epicardium. Also shown are different positions of the lead tip, including inadequate fixation, proper fixation and full perforation.

2.4 Performing Perforation Tests

In order to understand the mechanisms that are at work when implanting a lead and when the heart wall is perforated tests can be performed. Based on the description of lead implantation and perforation risk such tests should be performed in the right atrial or right ventricular tissue. The largest tissue sample is usually easiest to obtain from the outer right ventricular wall.

In order to investigate the strength of the heart tissue, perforation tests can be performed. Different methods are possible. Method A in Figure 2.6 is a method that allows for performing several well-controlled perforation tests on the same piece of tissue. Method B is more similar to the perforation situation in the real heart, but is more difficult to control. Method A was the method used for the perforation tests that are analyzed in this thesis.

Instead of using a full lead during these tests only the distal, rigid portion, of the lead is used. In some cases, it may not be possible to use a real lead at all and then a mechanical model that mimics the mechanical dimensions of the tip of the lead is manufactured. This is called a *punch* in this report. The punch can be more or less equal to the tip of a real lead. For instance, it may or may not have a helix and it may be shaped like a tube or like a solid cylinder.

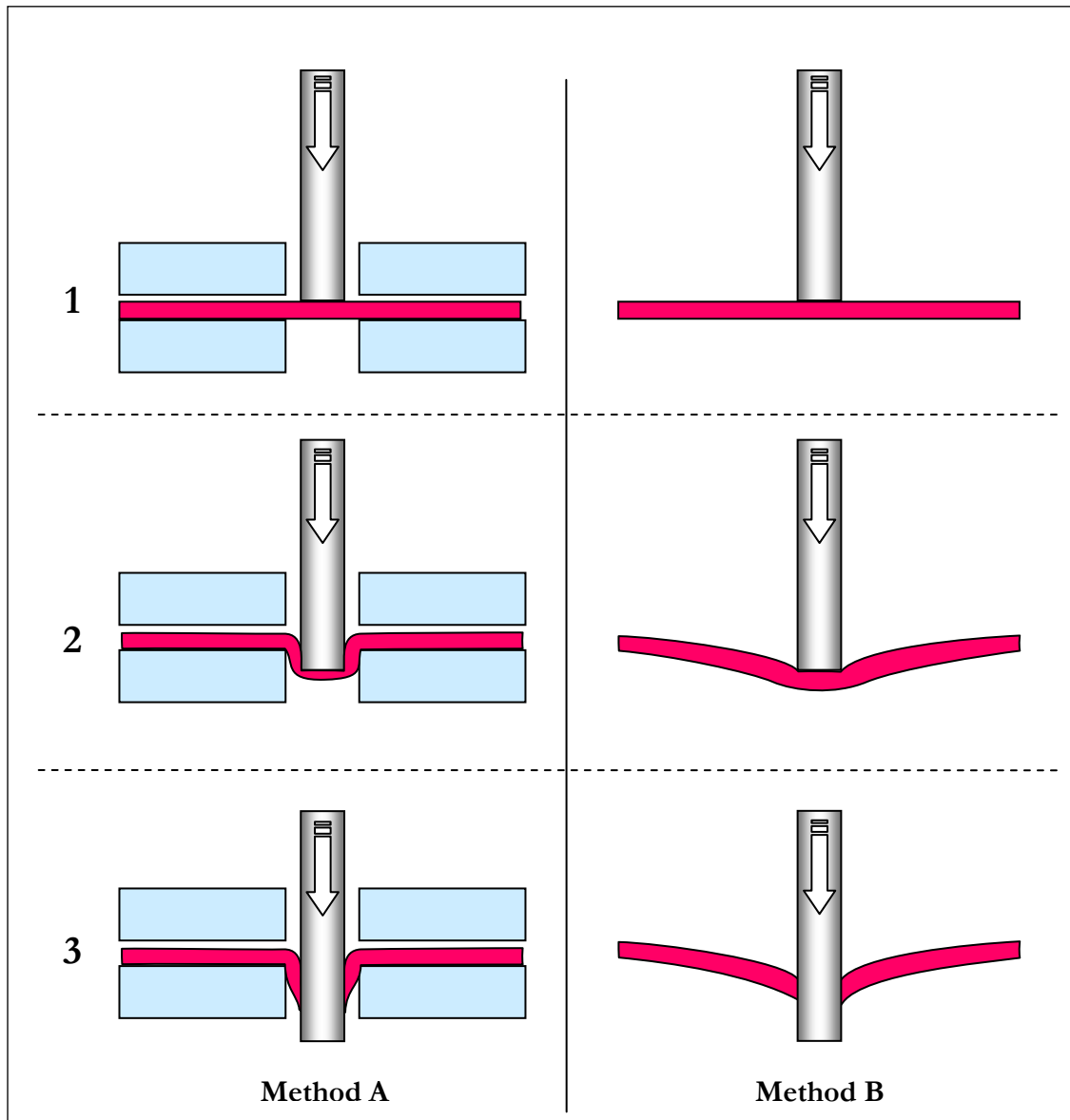


Figure 2.6: The figures to the left show perforation using a fixture to hold the tissue during perforation. The figures to the right show the case where the tissue is only held at the edges and is allowed to flex freely in the middle. In both cases the upper figure (1) shows the punch before it comes into contact with the tissue, the middle figure (number 2) shows the punch when it is applying force to the tissue, but before full perforation and the lower figure (number 3) shows the punch after it has penetrated the tissue.

The perforation itself is performed by moving the punch slowly, with constant speed in a quasi-static fashion, towards the tissue as shown in Figure 2.6 until the tissue has been fully perforated. During this motion, the opposing force that is sensed by the punch is measured. An example of such a force curve is shown in Figure 2.7, with the different positions 1, 2 and 3 indicated.

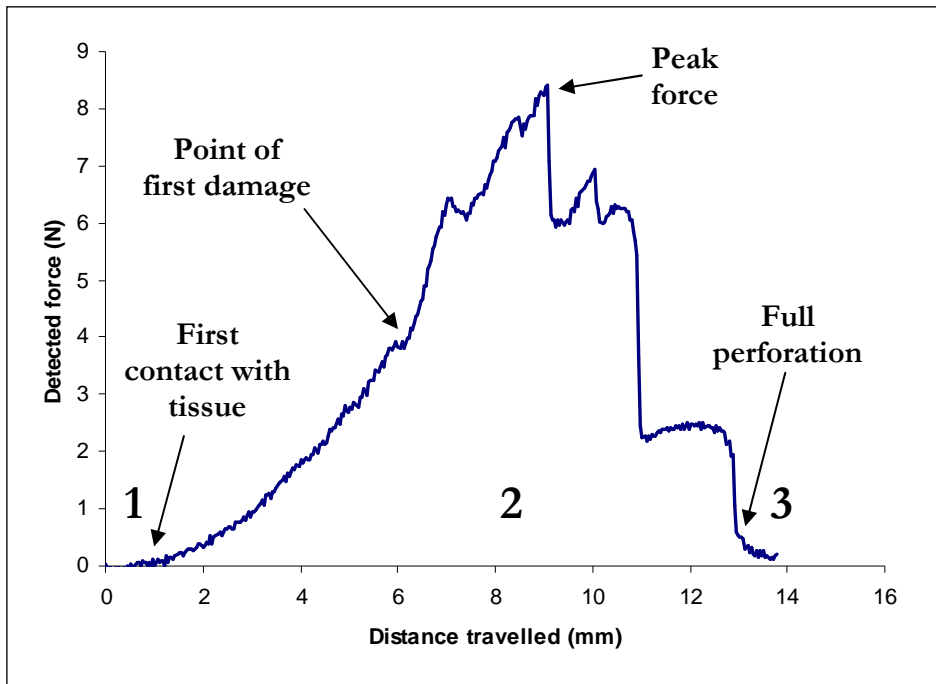


Figure 2.7: The figure shows a typical perforation curve, where the measured force has plotted versus the distance travelled during a full perforation of porcine cardiac tissue. The numbers 1, 2 and 3 represent the same three positions of the punch as in Figure 2.6. During the first smooth portion of the curve no damage has yet occurred. Between the first damage and full perforation, the punch goes through first the endocardium, then the thicker myocardium and finally the epicardium.

2.5 Use of Porcine Tissue

Because of ethical reasons, it is not easy to perform tests on human heart tissue, even if this would be preferred from a scientific standpoint. Instead, alternatives are used. Porcine heart can be used as a substitute, and are often used in the testing of pacemaker leads. Hearts from pigs are also readily available.

2.6 Terminology and Abbreviations

pacemaker	Electrical device that can pace the heart artificially if the hearts own function for pacing is not adequate or fails completely. It is connected to the heart via a lead, an electrical cable.
ICD	Implantable Cardioverter-Defibrillator. A device that functions similarly to a pacemaker, but with additional capability to defibrillate the heart using a high voltage pulse to regain normal heart function if the heart is beating much to fast in an uncontrolled manner, a flutter or a fibrillation.
the device	A common name for either a pacemaker or an ICD.
lead	The electrical wire that connects the device with the heart.
French	Unit of measure for the diameter of the lead. Abbreviated F. 1F is <i>approximately</i> 1/3 mm, so a 6F lead is about 2 mm in diameter.
distal end (of lead)	The end furthest away from the device. This end contains the electrodes and is implanted in the heart.
proximal end (of lead)	The end closest to the device. This end has a connector that connects electrically and mechanically to the device.
header	The distal part of the lead. For active leads, the header houses the helix and helix mechanism.
helix	The helix is a spiral shaped wire that extends from the tip of the lead and that attaches the lead to the heart wall like a corkscrew. It also serves as an electrode, connecting the lead electrically to the heart.
penetration	In this context used when an object enters the heart wall but does not go completely through it.
perforation	In this context used when an object goes completely through the heart wall.
quasi-static	In this context, this means that the motion during the perforation is so slow that no dynamic effects occur.
punch	Device used to perform the perforations. Designed to resemble the lead tip or the entire header of the lead.

3 Key Questions

Based on initial considerations regarding what knowledge might contribute to our understanding of heart wall perforations the following questions were identified as being most important to address in the analysis:

No	Question	Details	Relevance
Q1	Is there a difference in force between different punches?	What is the relationship between the force and the diameter? Does the hollow tube give a larger or smaller force than the solid cylinder? Does the helix increase or decrease the perforation force?	The main purpose of the original thesis [2] was to answer these questions. Here they are addressed using statistical methods.
Q2	What is the statistical distribution for the measured force values?	Is it normally distributed or does some other distribution give a better fit?	Important for building a statistical theory about the strength of heart tissue. Can help in understanding real perforation data.
Q3	Is the tissue homogeneous?	Are different positions independent of each other or are there stronger/weaker areas?	May allow this test method to be used for mapping the strength of the heart. Important also to understand the results of the testing performed in [2].
Q4	Are different pieces of porcine tissue "equal"?	Do they have the same distribution (average, standard deviation, homogeneity etc)?	This affects how much one should rely on test data coming from only a single piece of heart tissue.
Q5	Does the tissue age during the test?	Does the force increase or decrease during the test? Do adjacent holes affect the force for new perforations?	If the tissue ages, extra care is needed when performing experiments so that the aging is not misinterpreted as a difference between punches.

Table 3.1. The table summarizes the key questions that this thesis investigates.

All of these questions are addressed in the next Chapters and the results have been summarized in Chapter 7.

4 The Performed Tests

In this Chapter we briefly describe the specifics of the performed perforation tests (Section 4.1), the tissue samples used (Section 4.2), the punch samples (Section 4.3) and the test equipment (Section 4.4). The information in this Chapter is described in more detail in [2].

4.1 Perforation Tests

For the tests that are analyzed in this thesis method A according to Figure 2.6 is used, i.e. the tissue is supported by plates above and below it and the punch is guided through holes in the plates. In total 99 perforations were performed for each piece of tissue as defined by the holes in the supporting plates (see Figure 5.1 and Figure 5.2). During the testing, a protocol was used and hand-written notes were taken. These notes indicate if the perforation was correctly performed according the protocol or not. Examples of incorrect tests are when the test was not fully completed so that the end of the registered force curve is missing or when the punch by mistake hit the edge of the holes in the supporting plates. The notes were used to define which perforations to include in the analyzed data material. Based on the randomness of such mistakes it is believed that these missing data do not affect the conclusions drawn from the analyzed data material.

4.2 Tissue Samples

Porcine heart tissue was used for the tests. The hearts were delivered directly to the test site and were stored at about $+5^{\circ}\text{C}$ in saline solution until the tests. The tissue samples were cut from the outer right ventricular heart wall and the perforations were performed from the endocardium side (the inner side). The pieces of tissue were approximately 8 cm x 8 cm. The tissue was stretched by about 12.8% in the longitudinal direction and 8.4% in the transverse direction to mimic the strain in a normally function heart [1].

During testing the tissue samples were surrounded by Saline solution, a water based liquid with salt content matching that of the human body. The solution and the tissue were held at approximately 37°C throughout the testing. Data from 14 hearts are analyzed in this report.

4.3 Punch Samples

Three different types of punches were used, with different radius:

- Solid punch: 3, 4, 5, 6, 7 and 8F.
- Tubular punch: 4 and 6F.
- Tubular punch with helix: 4 and 6F.

Here F means “French” which is a measure of the diameter of a cardiac lead. For reference, 6F is approximately 2 mm.

During the perforation tests focus was mainly on the solid and the tube-shaped punches, but some tests were also performed with the tube shaped punches with a helix. This last type is most similar to active leads with the helix extended, but because of limitations of the punch samples that were available during these tests, not too many tests could be

performed with these. Therefore, this analysis will mainly focus on comparing the solid and tube-shaped punches and looking into the effect of the diameter of the punch.

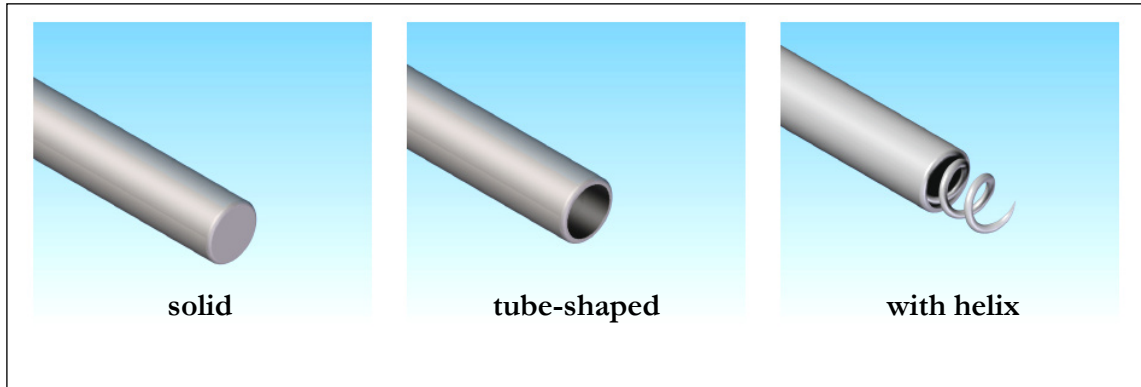


Figure 4.1. Distal part of the punches used⁴. The punch with helix is most similar to the standard active lead with the helix extended, while the solid and tube shaped punches are similar to the lead with the helix retracted.

4.4 Test Equipment

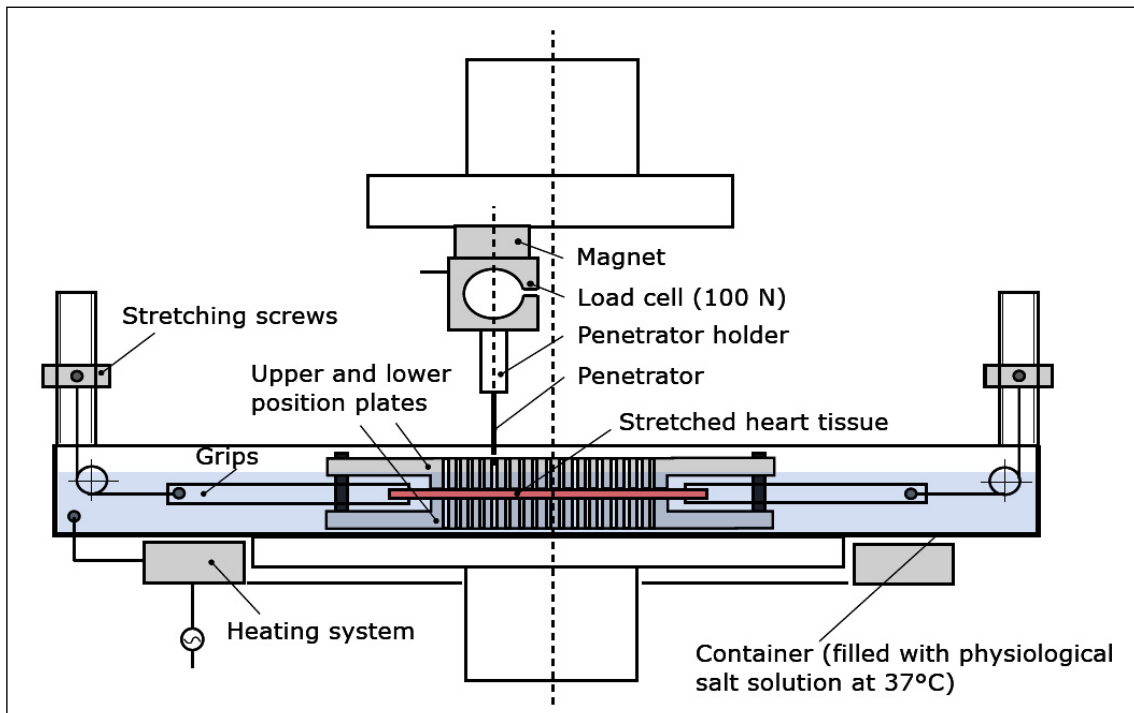


Figure 4.2. Schematic drawing⁵ of the experimental device used to penetrate bi-axially stretched specimens of ventricular tissue.

⁴ Adapted from figure 3.4 in [2].

⁵ Copied from figure 3.2 in [2].

The test equipment was semi-automatic. Positioning of the punch was manual, but the penetration was performed automatically with a penetration speed of about 5 mm/minute. When moving this slow the perforation is considered quasi-static, i.e. no dynamic effects occur. One complete perforation took about 3-4 minutes to perform from positioning to full perforation of the tissue. During the perforation procedure, the force detected by the punch was continuously measured by a load cell and simultaneously the distance travelled was logged. The data for each perforation was stored to a separate file for later analysis.

5 The Data Material

This Chapter gives an overview of the analyzed data material (Section 5.1) and discusses the randomization used during testing (Section 5.2). The two analyzed parameters, the peak force and the force at first damage to the tissue, are defined (Section 5.3) and the method for extracting them from the raw data is described (Section 5.4). The specifics of manually identifying the point of first damage are documented to give the reader a better understanding for this parameter (Section 5.5).

5.1 Overview

Table 5.1 summarizes the available data.

Tissue Sample ID	Punch Type, Size in French										Comment
	Solid						Tube		Helix		
	3	4	5	6	7	8	4	6	4	6	
P4RO	25 (0)	23 (2)	-	-	24 (1)	24 (0)	-	-	-	-	Not randomized order.
P5RO	22 (3)	23 (2)	-	-	25 (0)	24 (1)	-	-	-	-	Not randomized order.
P6RO	21 (4)	25 (0)	-	-	25 (0)	20 (4)	-	-	-	-	Not randomized order.
P7RO	-	-	23 (2)	25 (0)	-	-	24 (1)	24 (0)	-	-	Not randomized order.
P8RO	-	24 (1)	-	25 (0)	-	-	25 (0)	23 (1)	-	-	Not randomized order.
P9RO	-	25 (0)	-	25 (0)	-	-	25 (0)	24 (0)	-	-	Not randomized order.
P10RO	-	25 (0)	-	25 (0)	-	-	25 (0)	24 (0)	-	-	Not randomized order.
P11RO	-	25 (0)	-	25 (0)	-	-	47 (2)	-	-	-	Randomized order and position.
P12RO	-	-	-	-	-	-	25 (0)	25 (0)	24 (1)	24 (0)	Randomized order and position.
P13RO	-	-	-	-	-	-	49 (1)	-	49 (0)	-	Randomized order and position.

Tissue Sample ID	Punch Type, Size in French										Comment
	Solid						Tube		Helix		
	3	4	5	6	7	8	4	6	4	6	
P14RO	-	-	-	-	-	-	48 (1)	-	47 (3)	-	Randomized order and position.
P15RO	22 (3)	24 (1)	-	-	24 (1)	22 (3)	-	-	-	-	Randomized order and position.
P17RO	-	24 (0)	-	20 (5)	-	-	25 (0)	23 (2)	-	-	Randomized order and position.
P18RO	15 (9)	22 (3)	-	-	20 (5)	21 (4)	-	-	-	-	Randomized order and position.

Table 5.1. The table summarizes the available test data. The sample ID indicates that the sample is porcine (P) and that it has been cut from the outer side of the right ventricle (RO). In this report, usually only the tissue number will be used to reference the tissue sample. The table shows the number of valid tests that were performed for each combination of tissue and punch. The number in parentheses indicates how many tests that were excluded. Data was excluded if it was clear from notes made during testing that a mistake was made or if inspection of the data showed that the perforation was not completed. Inspection of the excluded data points does not indicate that the exclusion affects the statistical analysis or the conclusions.

As can be seen the data has not been collected according to a balanced design. This means that F-tests within the scope of variance analysis may not be exact; and tests for any interaction between factors will require the selection of data sets that include all combinations of the factors. We will see examples of this in the analysis in Chapter 6.

5.2 Order of Perforation and Randomization

As indicated in Table 5.1 the first half of the test data was not collected in a randomized fashion. The perforation matrix for these tests can be seen in Figure 5.1. As can be seen punch A was used for the entire piece of tissue first (numbers 1-25), then punch B (numbers 26-50) and so on. This means that aging of the tissue (or other similar effects) could affect the collected data.

A better way of performing the perforations is to randomize the order in which the punches are used. This method was used for the final tests and can be seen in Figure 5.2. This is a randomized perforation matrix in terms of the order in which the punches are used. The punches are well spread over the entire tissue.

Note that for tissue sample 11 only three punches were used and for tissue samples 13 and 14 only two punches were used. For these tissue samples, the same punch was used for two of the letters A-D in Figure 5.2 so that the total number of perforations was still approximately 99 for each tissue sample. Which of the punches that were used more than one time, can be seen by inspecting Table 5.1 for punches that were used more than 25 times on a single piece of tissue.

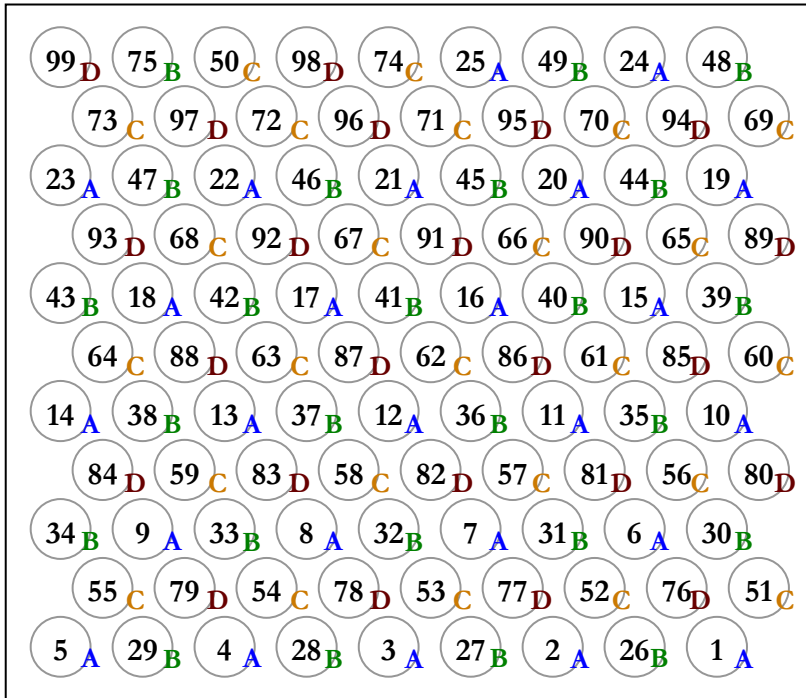


Figure 5.1. Perforation matrix for tissue samples 4, 5, 6, 7, 8, 9 and 10. The letters A, B, C and D represent the different punches used. The numbers show the order in which the perforations were performed. The order of the punches is not randomized.

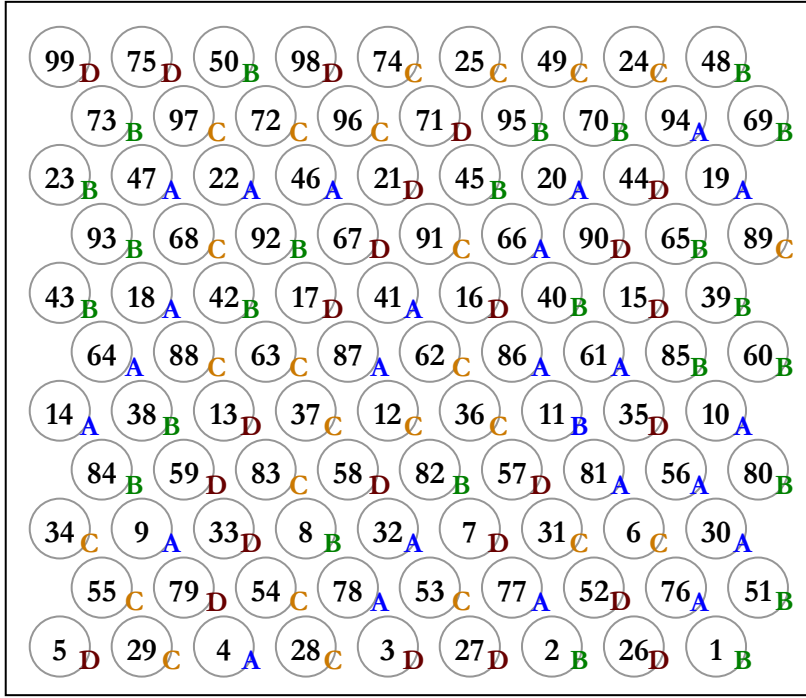


Figure 5.2. Perforation matrix for tissue samples 11, 12, 13, 14, 15, 17 and 18. Here the order of the punches is also randomized. Note that for tissue samples 11, 13 and 14 not all of the positions (A, B, C and D) were used for different punches, but some of the positions were used with the same punch.

5.3 Extracted Parameters

For each perforation a number of parameters were extracted or calculated from the raw data. For this thesis, two parameters were selected as most relevant:

- F_{peak} The peak force (the highest force value obtained during the perforation).
- F_{jd} Force at first damage. The point where the curve first deviates from elastic deformation.

The definition of these parameters can be seen in Figure 2.7 and more examples can be found in Figure 5.3 and Figure 5.4.

5.4 Software for Extraction of Parameters

In order to view the data more easily and to extract the parameters a program was written in Matlab. The program has a graphical interface that is shown Figure 5.3. This program was used to inspect the data to see if the perforation was completed, if there were any anomalies and finally to visually identify the position of the first damage.

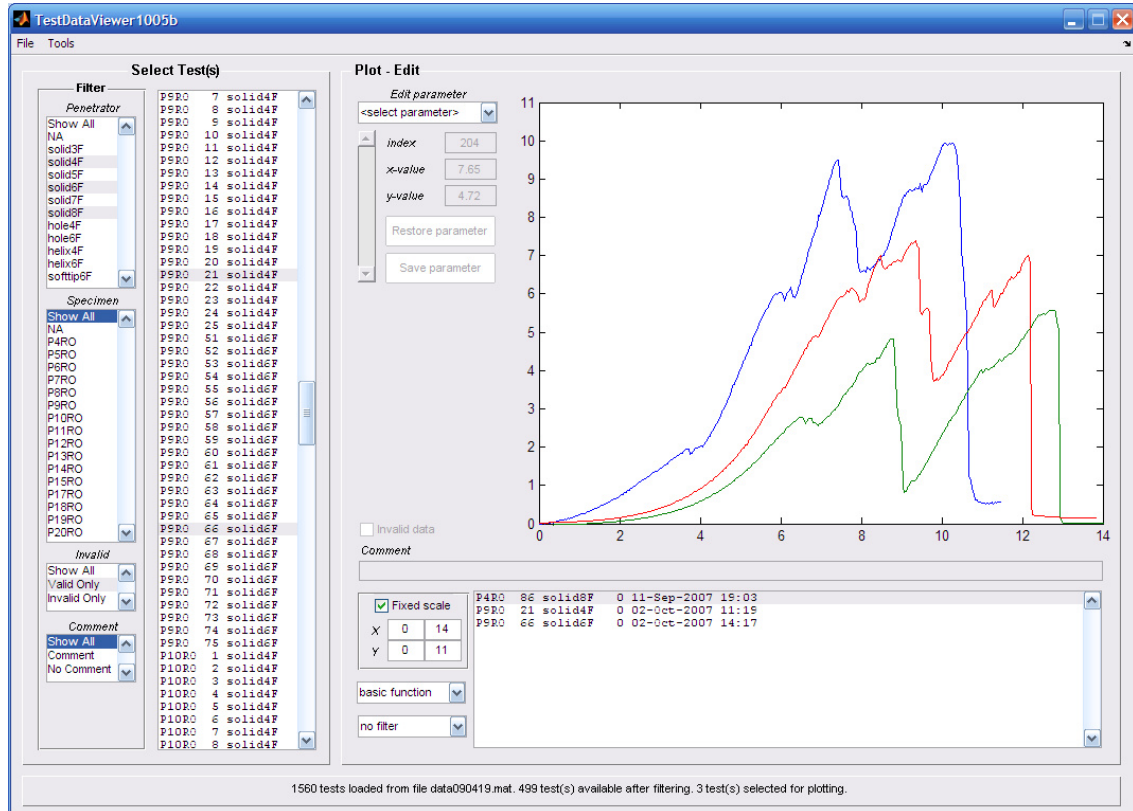


Figure 5.3. Sample view of the interface to the data viewer application. As can be seen several perforations can be selected at the same time facilitating easy comparison between different perforations. The example shows a solid 4F, 6F and 8F punch.

5.5 Identification of the Point of First Damage

The point of first damage is important as this allows us to perform a statistical analysis for how much force can be applied before irreversible damage occurs to the tissue. This has

clinical relevance since it is preferred not to inflict any damage, except when the helix attaches to the tissue. The definition of first damage that we use here is similar to the limit between the *elastic deformation* and the *irreversible deformation* as defined in [1]. This point of first damage could be possible to extract using some type of automatic computerized algorithm, but such an algorithm may be difficult to construct in practice. For this thesis, the identification of the point of first damage was done visually only. It was defined as the position where the curve *visually* deviates from the smooth elastic deformation curve. Figure 5.4 shows some typical examples.

Regardless if the extraction is automatic or is purely visual, the point of first damage defined in this way has not been correlated with actual damage to the tissue. However, it is still relevant as a method to *estimate* at what force initial damage to the tissue can occur. This can help establish limits for the maximum force the lead is allowed to apply to the tissue. This is a better limit than just looking at the peak force, since it gives some margin to the force at which full perforation occurs.

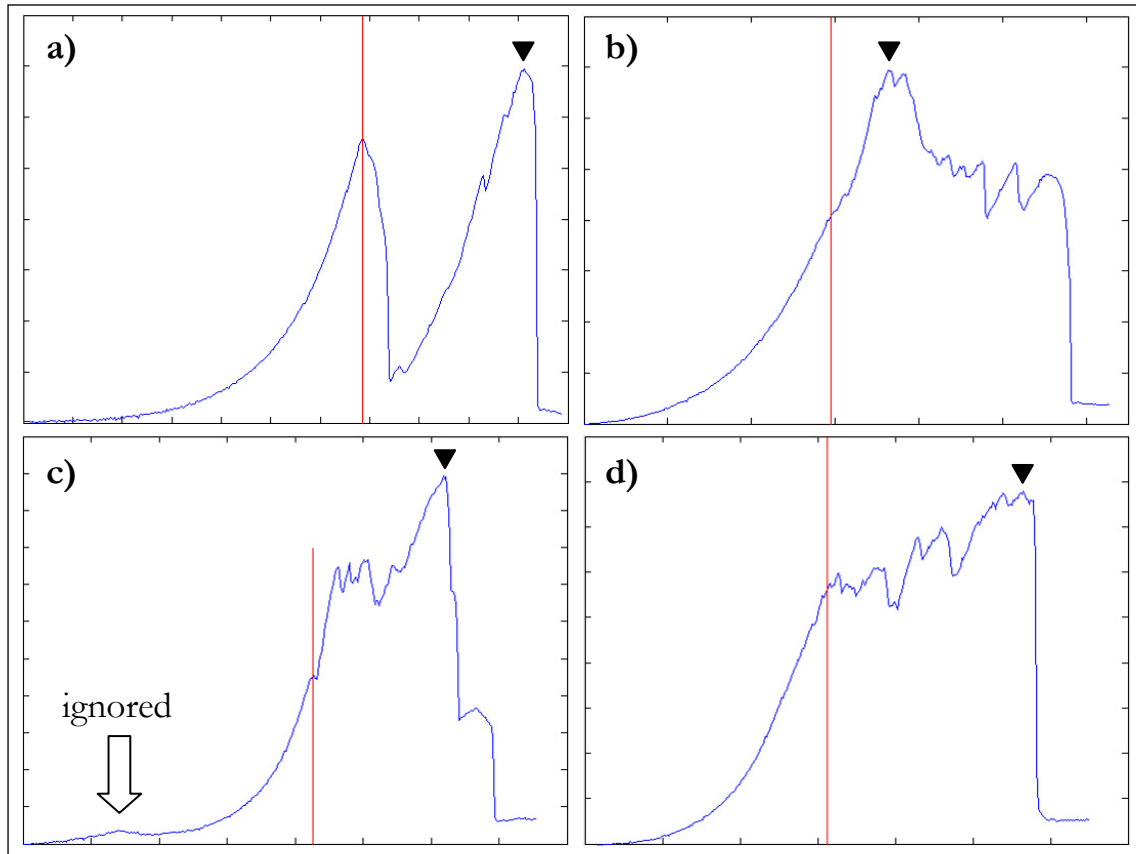


Figure 5.4. Identification of the point of first damage (vertical line) and peak force (triangle). a) Clear indication of perforation of endocardium (first damage) and also clear indication of peak force. b) Indication of deviation from elastic curve. c) Deviation from elastic curve, and ignored early deviation from elastic curve (see arrow). d) Clear deviation from elastic curve. Note that in all of these examples the peak force is higher than the force at indication of first damage. In the full data material, in some cases they were the same, but the peak force can of course never be lower than the force at first damage.

6 Statistical Analysis

In this chapter, we analyze the data with the purpose of answering the key questions defined in Chapter 3. The analysis is done in several steps, not necessarily starting with the most important question.

Here we start by looking at the individual pieces of tissue to see if they can be said to be homogeneous or not. We do this by defining a correlation coefficient that is analogous to Pearson's correlation coefficient, but not identical with it. Using this correlation coefficient and graphical plotting of the standardized force we show that some of the tissue samples are heterogeneous, with stronger and weaker areas, and that in general the correlation coefficient is positive (Section 6.1).

Since half of the data was not collected in a fully randomized fashion we also need to establish if all the data can be used in the analysis or if we need to exclude it or correct it in some way. We show that there is no indication of any aging effect for the tissue, or of any interaction between different perforation rounds, and that all data therefore can be used in the analysis (Section 6.2).

We continue with a brief analysis of the limited data with and without a helix to show that in general the helix decreases the perforation force. We also see that there is an interaction between the tissue and punches with and without a helix (Section 6.3).

We then arrive at the most important part of the analysis where we analyze all of the test data, excluding the helix data. We see that the median force is roughly linearly dependent on the diameter and that the tubular punch gives a higher force than the solid cylindrical punch. (Section 6.4).

We complete the Chapter with a discussion regarding distributions, specifically the logarithmic transformation of data, which results in approximately normally distributed residuals (Section 6.5).

6.1 Assessment of the Homogeneity of the Porcine Tissue

We wish to establish if the tissue is homogeneous or if there are stronger or weaker areas in the tissue. Based on how heart tissue looks and feels we intuitively expect the tissue not to be homogeneous, but we would prefer to have a method to test this. Here we define such a method (Section 6.1.1) and apply it to the porcine data (Section 6.1.2) and, using statistical tests, we find out that the porcine tissue is indeed not homogeneous. This is illustrated graphically (Figure 6.3) for tissue sample 10 which is most heterogeneous according to this method. Finally, also other methods of assessing the homogeneity of the tissue are discussed (Section 6.1.3).

6.1.1 Defining the Correlation Coefficient for the Tissue Samples

We start the analysis by investigating the pieces of heart tissue individually. Specifically we address the question if the tissue can be said to be homogeneous or not, that is if the force is uniform over the tissue or if it is spatially correlated. In the following discussion, we will call each perforation position a *node*. We define a correlation coefficient in such a way that if the peak force measurements are randomly distributed over the nodes the correlation coefficient will be close to zero.

First, we need to take into account that each piece of tissue has been perforated by up to four different punches. We cannot expect these to have the same mean or the same standard deviation in terms of force. Therefore, we cannot set out to define a correlation coefficient based on the raw force data that we collected. We need to transform the data in some way. We can do this if we first make the following observation: Both for the randomized and the not fully randomized tests the punches are evenly spread over the tissue. We can expect them to “sample” the tissue in the same way. This leads us to the following important assumption:

- Each punch spans the entire tissue in such a way that if the punches A, B, C, D had been identical they would have had the same expected mean force and the same expected variance.

Using this assumption, we select the proper transformation to be a standardization of the data individually for each piece of tissue and punch. Typically, each group will consist of approximately 25 force values, and therefore mean force for the group will not be too sensitive to single deviating force values.

We will call this new standardized force data set z_i . Now we are ready to define the correlation coefficient for the tissue.

We start with the familiar expression for Pearson’s *sample correlation coefficient* [4]:

$$r_{xy} = \frac{\sum (x_i - \bar{x})(y_i - \bar{y})}{(n-1)s_x s_y} \quad (6.1)$$

In this special application, we need to do some adaptations. First, we perform a sum over all pairs of neighboring nodes. In this case, we define neighboring nodes to be the six closest nodes as shown in Figure 6.1.

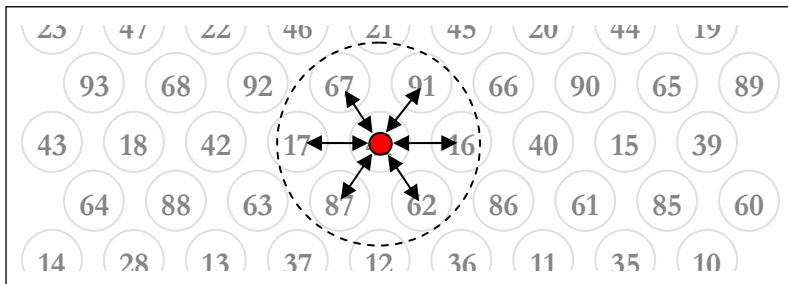


Figure 6.1. For each penetration position (node), we calculate the “correlation” with adjacent nodes. Here we only look at the six closest nodes and call these the neighbors of the selected node. At the edges or when data points are missing, some nodes will have fewer neighbors. To calculate the correlation coefficient for the tissue we perform this type of summation over all the nodes on the tissue. This is done in a way that is analogous to Pearson’s “sample correlation coefficient”.

We will work with what could be called a bi-directional relationship between nodes. This is an arbitrary, but logical choice, since there is no reason to prefer one node to another. This way of defining the summation will create a symmetrical equation, which simplifies the formulas and the calculations. The symmetry results in each node appearing in both the

”x”-set and the ”y”-set in equation (6.1), making the two sets identical, except for the ordering of the nodes.

Using our standardized data set z_i , we arrive at the following expression for the correlation coefficient:

$$r_z = \frac{\sum_{i=1}^N \sum_{j \sim i} (z_i - \bar{Z})(z_j - \bar{Z})}{(\tilde{N} - 1)S_z^2} \quad (6.2)$$

Here the used symbols are defined in the following way:

N	The total number of data points for a specific piece of tissue.	If all perforations successfully resulted in a measured peak force then this is equal to 99, but in general it is less slightly less than 99 (se Table 5.1).
z_i & z_j	The standardized data points for a specific piece of tissue. The standardization is performed individually for each punch.	$i, j = 1, 2, \dots, N$.
$j \sim i$	Each node j that is a neighbor of node i .	Here we have defined the neighbors to be the six closest nodes in a geometrical fashion. At the edges, or where data points are missing, there may be fewer neighbors. Some nodes may completely lack neighbors if several data points are missing and will thus not be included in the summation.
\tilde{N}	$\tilde{N} = \sum_{i=1}^N \sum_{j \sim i} 1$	The total number of neighboring nodes.
\bar{Z}	$\bar{Z} = \frac{1}{\tilde{N}} \sum_{i=1}^N \sum_{j \sim i} z_j$	Mean of all neighboring nodes and not identical to \bar{z} , which is the mean of all data points for a piece of tissue.
S_z^2	$S_z^2 = \frac{1}{\tilde{N} - 1} \sum_{i=1}^N \sum_{j \sim i} (z_j - \bar{Z})^2$	The sample variance for the neighboring nodes, analogous to the sample variance we are familiar with from basic courses in statistics (se reference [4] for the normal definition of sample variance).

Some additional algebra yields:

$$r_z = \frac{\sum_{i=1}^N \sum_{j \sim i} (z_i - \bar{Z})(z_j - \bar{Z})}{(\tilde{N} - 1)S_z^2} = \frac{\sum_{i=1}^N \sum_{j \sim i} z_i z_j - \tilde{N} \bar{Z}^2}{\sum_{i=1}^N \sum_{j \sim i} z_j^2 - \tilde{N} \bar{Z}^2} \quad (6.3)$$

The actual calculation is computerized via programming in Matlab. The algorithm involves standardizing the data for each punch on a piece of tissue, and then performing the summations according to equation (6.3). We arrive at a single number for each piece of tissue that characterizes the tissue in terms of internal correlation of the force between neighboring nodes.

To understand the correlation coefficient more intuitively we can start with equation (6.3). We see that the denominator is merely a measure of the variation in the data as a whole, so we ignore it. For standardized data we also see that $\tilde{N}\bar{Z}^2$ will be close to zero, so we ignore it also. What remains is a sum over $z_i z_j$. Now it is easy to realize that if neighboring nodes are similar they will both be positive or both be negative. In both cases the product will be positive and the numerator will tend to be positive, so the correlation coefficient will be positive. If neighboring nodes tend to have opposing values, then $z_i z_j$ will tend to be negative and so the correlation coefficient will be negative. Finally, if the neighbors are not correlated, then $z_i z_j$ will sometimes be positive and sometimes negative, resulting in a value close to zero for the correlation coefficient.

6.1.2 Calculated and Simulated Values of the Correlation Coefficient

The calculation defined above is performed separately for the peak force and for the force at first damage.

Tissue #	Correlation coefficient, r_z	
	for peak force	for force at first damage
4	0.125	0.010
5	0.122	0.105
6	0.070	0.090
7	0.271	-0.031
8	-0.056	0.055
9	0.296	0.161
10	0.469	0.324
11	0.174	-0.002
12	0.132	0.123
13	0.100	-0.030
14	0.093	0.024
15	0.083	0.082
17	0.386	0.077
18	0.180	0.412

Table 6.1: Calculated correlation coefficient r_z for each piece of tissue using the algorithm described above. Calculations have been performed both for the peak force and for the force at first damage. By inspecting these values we see that in general they are positive, more so for the peak force than the force at first damage. This means that the correlation coefficient is in general positive, which could be an indication of heterogeneity in the tissue. The “worst” tissue samples are sample 10 for the peak force and sample 18 for the force at first damage.

In order to understand if these numbers are high or low, extreme or as expected, we need something with which to compare them. We can do this by simulating randomly

distributed, uncorrelated tissue. Using Matlab, we generate random, independent force values for each node on the tissue. For simplicity, we use all the 99 available nodes. We then allow the previously described algorithm to calculate a “simulated” correlation coefficient for each such simulated piece of tissue. To make sure that the chosen distribution for the simulated data does not affect the result we simulate data from two different distributions, the normal distribution and the exponential distribution. Since the data is standardized in the algorithm performing the calculation of the correlation coefficient, we do not need to bother about exact parameters of the distributions – it is merely the shape of the distribution that affects the behavior of the correlation coefficient. For instance, for the normal distribution we simply select $N(0, s^2=1)$ distributed data.

Using the algorithm described above we have simulated 100 000 tissue samples, which have then been plotted in a normal chart together with the real porcine tissue correlation coefficients.

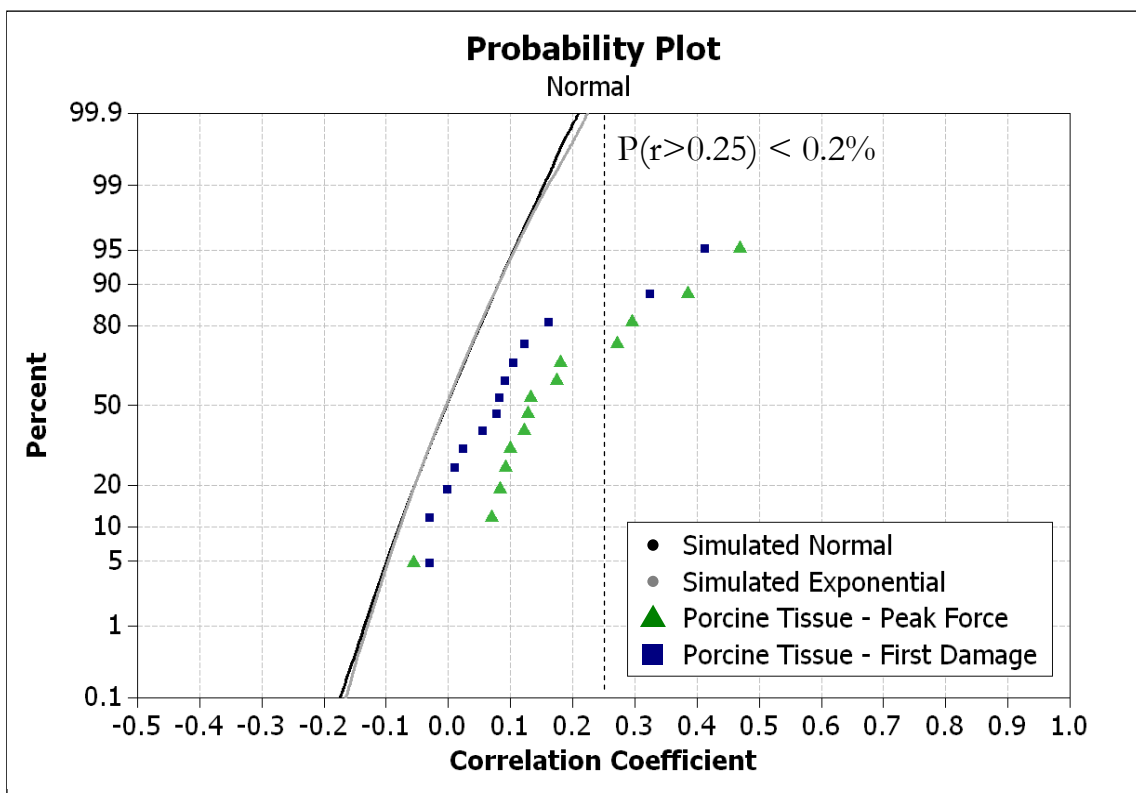


Figure 6.2. The triangles and squares correspond to actual correlation coefficients for the porcine tissue samples. These values can be compared with simulated tissue samples with simulated independent, random force data. The black dots (forming a black line) come from simulating from the normal distribution and the grey dots (forming a grey line) come from the exponential distribution. As can be seen the lines overlap over a great portion of the range, so the distribution of the individual force values does not greatly affect the distribution of the correlation coefficient when the individual data points are truly uncorrelated. As a contrast, it can be seen that the correlation coefficients for porcine data are shifted to more positive values. The dashed line indicates the correlation coefficient 0.25 and is explained in the text.

From Figure 6.2 it can be seen that the porcine data is shifted towards higher correlation coefficients compared to the uncorrelated simulated data. It also appears that the peak force in general shows higher correlation coefficients than does the force at first damage. This can also be tested statistically; here we will use a nonparametric statistical method.

We first investigate if the median correlation coefficient is significantly higher than zero. We do this as a one-sided test based on the reasoning that it is unlikely that our defined correlation coefficient could detect a negative correlation coefficient (see also Section 6.1.3). Since we perform two tests for the two different measurements of force, we use Bonferroni correction when performing these tests at the simultaneous 5% level. We therefore end up with individual 2.5% levels for each of the tests.

We use the Sign Test [4], since we cannot assume that the distribution for the correlation coefficient is symmetrical around zero, and arrive at the following results:

Sign test of median = 0 versus > 0

	N	Below	Equal	Above	P	Median
r(peak force)	14	1	0	13	0.0009	0.1300
r(first damage)	14	3	0	11	0.0287	0.0797

Table 6.2: Result of Sign Test for the correlation coefficients.

From the analysis, we see that for the peak force we reject the hypothesis that the tissue is homogeneous, while for the force at first damage we cannot do this, at least not on the simultaneous 5% level.

There is also a second test we can do and that is to investigate which of the tissue samples are heterogeneous on the simultaneous 5% level. We do this, again as a one-sided test, by comparing each individual r-coefficient with the simulated distribution for the correlation coefficient. Here we will perform a total of 28 comparisons and so use Bonferroni correction to arrive at the individual $5\%/28 = 0.2\%$ level.

From the gray and black lines, we see that the probability to get a correlation coefficient that is **larger** than 0.25 is clearly less than 0.2%. We now see that six of the correlation coefficients are larger than this and conclude that in these six cases we can reject the null hypothesis that these are the product of homogeneous tissue.

These tissue samples are:

- Peak force: sample 7, 9, 10 and 17.
- First damage: sample 10 and 18.

As a continued analysis, it is interesting to see what causes the higher correlation coefficient. We do this for one tissue sample only, the one with the highest correlation coefficient, tissue 10. There are at least two alternatives for the cause of the higher correlation coefficient:

- some smaller part of the tissue shows a higher or lower force than the rest of the tissue,
- the tissue has some more general structure, e.g. the force gradually increasing from one side of the tissue to the other.

We will explore which alternative is correct for this tissue sample graphically.

We use the same data that was used for the correlation coefficient (standardized per punch) and plot this in a shaded plot with spline functions between perforation points (black dots in the figure). The level of shading reflects the force level of that part of the tissue.

From the plot, it can be seen that the higher correlation coefficient for sample 10 is caused mainly by an area of higher force level at the bottom of the tissue (as drawn in Figure 6.3). This means that it is a smaller area that deviates from the rest of the tissue. There does not seem to be any corresponding weaker areas, but this has not been fully explored in this thesis. Such weaker areas would be of interest, as they would directly affect the probability of perforation of the tissue in the clinical implantation situation.

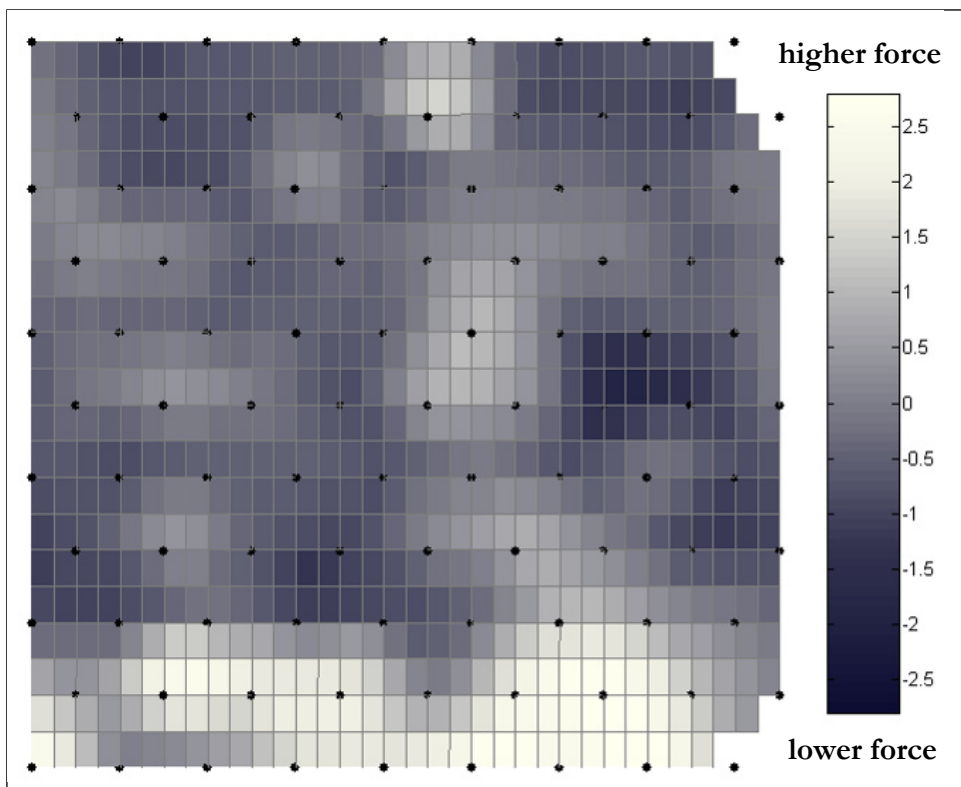


Figure 6.3. This is a graphical representation of the standardized force level for tissue sample 10 which has the highest correlation coefficient ($r_{\text{peak}} = 0.47$). Lighter and darker areas indicate a higher and lower standardized force, respectively. The scale can be found to the right in the figure. As it turns out the high correlation coefficient for tissue sample 10 is mainly caused by a stronger area on one side of the tissue (the lower part in the figure). The black dots in the figure represent the positions of the actual measurements. The shading has been created by Matlab as a spline surface that goes through all of the actual standardized force values in the indicated measurement positions. This graph is best viewed in “3D”, which gives an intuitive feeling for the force distribution over the tissue when rotated in 3D in real time. For printing the camera angle has been selected to create a “flat” image, as this is the best format for print.

6.1.3 Other Possible Tests and Transformations

Other ways of standardizing the data were also tested, like only subtracting the average, or subtracting the median instead of the average, but the correlation coefficients did not change much. In addition, a logarithmic transformation of the data was tested, in line with the transformation that is used later in this thesis, but this did also not affect the results much. The conclusions are the same and only the standardized data without any other transformation are used in this thesis.

The sensitivity of the correlation coefficient to structures in the tissue was also tested. This is important since we want the correlation coefficient to deviate from zero if the tissue is not homogeneous. If it does not vary, or varies in an undesired way, it is not a good statistic to use when testing for the homogeneity of the tissue. Both negative and positive spatial correlations were tested. The negative correlation was created by assigning forces with opposite sign to adjacent rows. The resulting correlation coefficient was approximately -0.5. It is likely that the correlation coefficient cannot be much lower when defined with six neighbors as shown in Figure 6.1, since this makes the two axes, x and y , dependant of each other. This is not explored further in this thesis. Note however that a true negative correlation coefficient would still be difficult to detect for a real piece of tissue since it requires the alternating pattern of the tissue to match the spacing and the positions of the perforations. In addition, positive spatial correlations were tested, both a second-degree function and a linear function and both yielded values close to (but slightly below) +1, which is to be expected. Detecting positive correlation coefficients does not require a close match between the tissue and the perforation positions.

This discussion shows that the defined correlation coefficient can be used to identify the existence of heterogeneity in the tissue samples, specifically when the heterogeneity consists of stronger and weaker areas in the tissue. Note that the size of such an area needs to be larger than the spacing between the perforation nodes in order to be detected. The test method cannot detect “micro structures” that are smaller than this spacing. This is analogous to sampling theory where similar limitations apply.

There are other methods to investigate if the tissue is homogeneous or not. One obvious method is to view this as a two factor experiment (the x and y -position for each tissue sample individually). We can then use regression (first or higher order polynomial, or some other arbitrary function) to see if any of the coefficients in the function turn out to be significant. If they do turn out to be significant we can conclude that there is indeed a structure and that the tissue is not homogeneous. However, the selection of such a polynomial or function would be entirely arbitrary and without a better theory of what the structure of the tissue should be the correlation coefficient together with the spline function and the graphical plot are sufficient.

6.1.4 Summary and Conclusions

We have defined a correlation coefficient for this type of tissue tests. This coefficient can be used to test if the tissue is homogeneous or not and, together with a color-grading plot, we can also determine the nature of the heterogeneity if the tissue is not homogeneous.

Using the calculated correlation coefficients and the color grading plot it was shown that the porcine tissue samples in general are heterogeneous having a median correlation coefficient for the peak force of about 0.13. Using statistical tests, we also specifically identified that four of the tissue samples are heterogeneous with respect to the peak force

and two with respect to the force at first damage. As an example, we saw that tissue sample 10 has a stronger area at the lower part of the tissue as shown in Figure 6.3.

One additional important conclusion regarding the positive correlation coefficient for the tissue samples is that this means that the individual perforation positions are not independent. This is briefly discussed in Section 7.2.

6.2 Does the Tissue Exhibit any Aging Effect?

We wish to use all the data that was collected in the perforation testing, but we know that not all of the data was collected in a randomized fashion (see Table 5.1). However if the tissue does not show any aging effect or similar, we can use data from the tests that were not randomized also, since then the order of perforation should not matter.

First, we define a statistical model capable of detecting aging of the tissue (Section 6.2.1) and then we analyze three sets of data (Sections 6.2.2, 6.2.3 and 6.2.4) to show that there indeed is no indication of such an aging effect during these tests. This allows us to use all of the data in the continued analysis.

6.2.1 Statistical Model

The data will be analyzed using a linear model approach. We then typically want the data to fulfill the following three criteria:

- 1) The error term should be normally distributed.
- 2) The distribution of the error term should be independent of the values of the parameters.
- 3) The individual data points should be independent.

This may require a transformation of the data if the error term is not normally distributed or if it does depend on the data. Here, we will use a logarithmic transformation of the force values, and this transformation is further discussed in Section 6.5.

We also note that the individual data points are not independent, since we found that the correlation coefficient for the tissue samples is in general positive (Section 6.1). We will ignore this in the continued statistical analysis, but note that the effect of this intrinsic tissue variation is added to the error term in the linear model.

We start the analysis of possible tissue aging by looking at how the test was actually performed. Each tissue sample was perforated in four rounds, each round roughly covering the same area (see Figure 5.1 and Figure 5.2). Thus for each round it should be possible to assume that if the tissue does not age, each round should show the same average force. We can test for the significance of the factor round by defining a linear model and creating an ANOVA-table. Here we assign the round as a third factor in addition to the tissue and punch factors.

However, we can only perform this test if the punches used for each tissue sample were randomized in order. This is true for the latter half of the samples (see Table 5.1 and Figure 5.2). Also, note that this test cannot be performed for a single round because of the way the penetrations were performed, in an ordered fashion from one side of the tissue to the

other. Any structure in the tissue could then show as a false aging effect. This could otherwise have been a better approach.

When performing this test we also need to check for any interaction between the different factors, as this might otherwise falsely show up as an effect of the round. By looking at the data as presented in Table 5.1, we see that we can perform this investigation, including any interaction effect, separately for the following three sets of data:

Data Set	Tissue Samples	Punches	Comment
1	12, 13 and 14	tube 4F and helix 4F	These are also the only tissue samples where the helix can be directly compared with the tubular punch. Significant effect of helix may be possible to detect.
2	11 and 17	solid 4F, 6F and tube 4F	Only a little variation in diameter, but can also compare solid and tube.
3	15 and 18	solid 3F, 4F, 7F and 8F	Only solid punch, but large variation in diameter. Significant effect of diameter expected.

Table 6.3. The table shows the three sets of data that will be used to test for aging of the tissue during the test.

We see that although not being balanced, each data set includes all the different punches listed for each tissue sample, including replicates. The fact that the tests are not balanced means that the performed F-tests in some cases will not be exact. Because of the reasonably large sample size for each combination of tissue and punch and because the number of tests for each combination of tissue and punch are comparable the F-test should still be reasonably accurate and should give a clear indication if an effect is significant or not.

For the analysis presented below the natural logarithm, $\ln(F)$, of the force was used instead of the original force, F . This is because the analysis itself and subsequent analyses show that this gives the best fit to the normal distribution for the residuals. This is further discussed in Section 6.5.

Using Minitab the same general linear model analysis was performed for each data set, starting with the following full model including interactions:

$$\ln(F_{ijkl}) = \mu + \alpha_i + \beta_j + \gamma_k + (\alpha\beta)_{ij} + (\alpha\gamma)_{ik} + (\beta\gamma)_{jk} + (\alpha\beta\gamma)_{ijk} + \varepsilon_{ijkl} \quad (6.4)$$

The parameters are the usual for this type of model⁶:

F_{ijkl}	The force	l is the index for the test within the group defined by a specific tissue, punch and round. The range for l is therefore different for each such combination. Indices should have been used to indicate this, but were omitted because this is obvious from the description of the data set (Table 5.1).
μ	The average of all data.	
ϵ_{ijkl}	The standard error term.	$\epsilon_{ijkl} \sim N(0, \sigma^2)$
α_i	The effect of the tissue, random factor.	$\alpha_i \sim N(0, \sigma_{\alpha}^2)$
β_j	The effect of the punch, a systematic factor.	$\sum_j \beta_j = 0$
γ_k	The effect of the round, a systematic factor (note that the order is not randomly chosen).	$\sum_k \gamma_k = 0$ $k = 1 \dots 4$ (representing the four rounds)
$(\alpha\beta)_{ij}$	The interaction between tissue and punch, a random factor since tissue is a random factor.	$(\alpha\beta)_{ij} \sim N(0, \sigma_{\alpha\beta}^2)$
$(\alpha\gamma)_{ik}$	The interaction between tissue and round, a random factor tissue is a random factor.	$(\alpha\gamma)_{ik} \sim N(0, \sigma_{\alpha\gamma}^2)$
$(\beta\gamma)_{jk}$	The interaction between punch and round, a systematic factor.	$\sum_j (\beta\gamma)_{jk} = \sum_k (\beta\gamma)_{jk} = 0$
$(\alpha\beta\gamma)_{ijk}$	The interaction between tissue, punch and round, a random factor since the tissue is a random factor.	$(\alpha\beta\gamma)_{ijk} \sim N(0, \sigma_{\alpha\beta\gamma}^2)$

For now, we are mainly interested in looking at significance, a full analysis the magnitude of the effects will be done later. The significance test was performed for all three sets of data and the results are presented in the next Sections with a summary Section at the end.

6.2.2 Analysis of Data Set 1

As can be seen in Table 6.10 this data set only includes a single punch diameter and the only difference between the punches is therefore the helix. Any detected effect of punch can therefore be attributed to the effect of the helix. Our main purpose is however to investigate if the factor round has any significant effect on the peak perforation force.

⁶ Minitab does not require the sum of random factors over indices of fixed factors to be zero. This does affect some of the F-tests. This has not been further explored in this thesis.

We start with the full model according to equation (6.4) and the result of the variance analysis is shown in Table 6.4. This result indicates that round is not an important factor. However, it also indicates that none of the factors are statistically significant except for a possible interaction between tissue and punch.

Inspection of the residuals shows that there are four large force values that deviate in terms of too large residuals. We perform the continued analysis without these four values and also remove the insignificant factors one by one. We end up with the result in Table 6.5.

We see that for this data set, there is only an interaction effect between the two tissue samples and the punches. Since the only difference between the punches was the presence or absence of a helix we conclude that there may be an interaction between punches with and without a helix and the tissue sample used. However, we do not find any significant effect of the round.

Analysis of Variance for log(Fpeak), using Adjusted SS for Tests

Source	DF	Seq SS	Adj SS	Adj MS	F	P
tissue	2	13.7896	13.9664	6.9832	6.46	0.141 x
punch	1	2.6130	3.3261	3.3261	3.21	0.214 x
tissue*punch	2	2.5944	2.1955	1.0977	6.35	0.033 x
round	3	0.1132	0.1918	0.0639	0.42	0.748 x
tissue*round	6	0.8877	0.9375	0.1563	0.90	0.548
punch*round	3	0.6262	0.3421	0.1140	0.67	0.598 x
tissue*punch*round	6	1.0390	1.0390	0.1732	1.46	0.193
Error	218	25.8525	25.8525	0.1186		
Total	241	47.5156				

S = 0.344368 R-Sq = 45.59% R-Sq(adj) = 39.85%

x Not an exact F-test.

Table 6.4. Analysis of variance for data set 1 using the full model for the peak force.

Analysis of Variance for log(Fpeak), using Adjusted SS for Tests

Source	DF	Seq SS	Adj SS	Adj MS	F	P
tissue	2	11.0904	11.1686	5.5843	3.52	0.221
punch	1	2.1927	2.8990	2.8990	1.93	0.298 x
tissue*punch	2	3.1712	3.1712	1.5856	15.40	0.000
Error	232	23.8897	23.8897	0.1030		
Total	237	40.3440				

S = 0.320894 R-Sq = 40.78% R-Sq(adj) = 39.51%

x Not an exact F-test.

Table 6.5. Analysis of variance for data set 1 using the reduced model for the peak force, with four high force values removed.

From the value of S, we can also calculate the random error to be approximately 40% ($e^{0.32}=0.38$) of the estimated force, which is quite large and forces us to use a large sample size to see any difference between punches.

An inspection of the residuals shows that, with the logarithmic transformation of the force, the resulting standard error is approximately normally distributed and seems to be independent of the fitted value; as is required by the linear model.

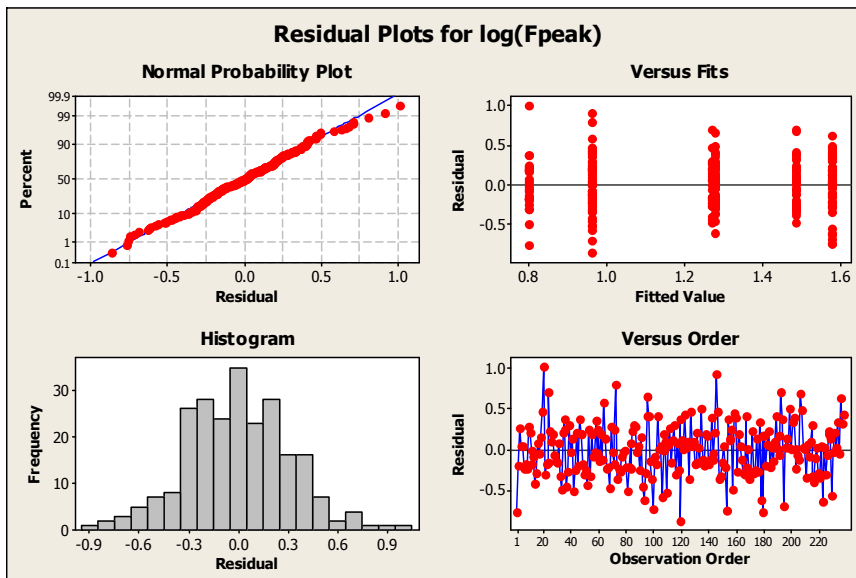


Figure 6.4. Residual plot for data set 1, for the reduced model for the peak force, with four high force values removed.

The same method was then applied for the force at first damage, with exactly the same conclusion, that there is an interaction between tissue and punch, but no effect of the factor round.

6.2.3 Analysis of Data Set 2

As can be seen in Table 6.3 this data set only includes punches with similar radius (compared to the full span of the punches used in the tests). Based on the large random error seen from the analysis of data set 2 we expect that it might be difficult to see any effect of punch in these tests.

We perform the analysis in the same way as for data set 1. Instead of showing all the steps, we only show the final model, with and without interaction with tissue and punch. As for data set 1, we have removed data points with a too high residual, in this case only one data point.

Analysis of Variance for $\log(F_{peak})$, using Adjusted SS for Tests

Source	DF	Seq SS	Adj SS	Adj MS	F	P
tissue	1	0.4257	0.2876	0.2876	6.25	0.121 x
punch	2	5.4138	5.2854	2.6427	58.81	0.017
tissue*punch	2	0.0899	0.0899	0.0449	0.34	0.714
Error	159	21.1935	21.1935	0.1333		
Total	164	27.1229				

S = 0.365093 R-Sq = 21.86% R-Sq(adj) = 19.40%

x Not an exact F-test.

Table 6.6. Analysis of variance for data set 2 using the reduced model, with interaction.

Analysis of Variance for $\log(F_{\text{peak}})$, using Adjusted SS for Tests

Source	DF	Seq SS	Adj SS	Adj MS	F	P
tissue	1	0.4257	0.2841	0.2841	2.15	0.145
punch	2	5.4138	5.4138	2.7069	20.48	0.000
Error	161	21.2834	21.2834	0.1322		
Total	164	27.1229				

$S = 0.363586$ $R\text{-Sq} = 21.53\%$ $R\text{-Sq}(\text{adj}) = 20.07\%$

Table 6.7. Analysis of variance for data set 2 using the reduced model, without interaction.

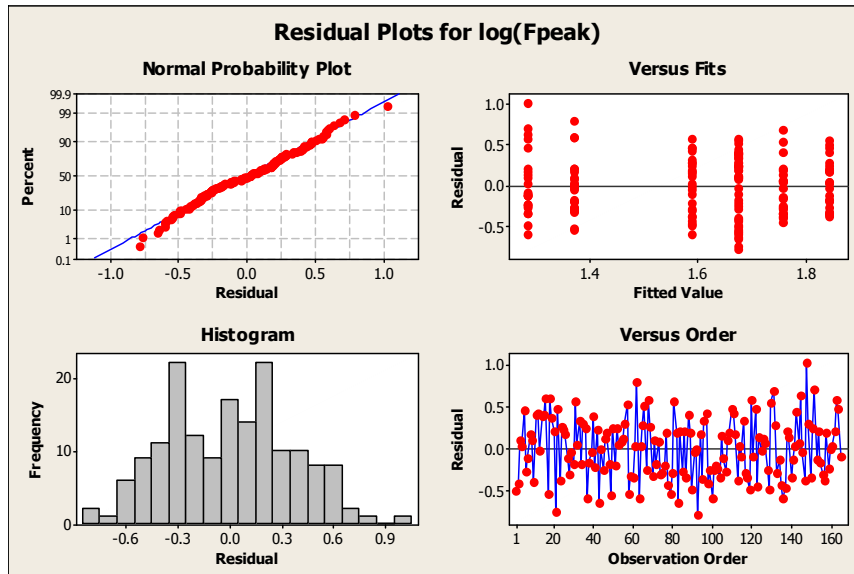


Figure 6.5. Residual plot for data set 2, for the reduced model, without interaction.

We see that only the punch shows any significant effect here ($p=0.000$ for punch and $p=0.145$ for tissue in Table 6.7), and in this case we can ignore the interaction between tissue and punch ($p=0.714$ for tissue*punch in Table 6.6). Quite contrary to the initial expectation, we see a clear effect of punch.

Something important to note for this data set is that R^2 , the degree of determination, is only about 20%, which is quite low. However, this is not so surprising since the punches are quite similar, and in this case, by chance the tissue samples turned out to be similar also.

The standard error is still approximately 40% ($e^{0.36}=0.43$) of the estimated force, and once again, the residuals are approximately normally distributed.

The same method was then applied for the force at first damage with the same result; that there is no effect of the factor round.

6.2.4 Analysis of Data Set 3

Finally, we turn to the last data set, which has four quite different diameters for the solid punches. Based on the previous results we expect to see a clear effect of punch, since the diameters differ so much. Using same procedure as before, with two data points removed, we get the following results (with and without interaction):

Analysis of Variance for $\log(F_{peak})$, using Adjusted SS for Tests

Source	DF	Seq SS	Adj SS	Adj MS	F	P
tissue	1	1.2228	0.6811	0.6811	5.27	0.104 x
punch	3	37.6172	36.9963	12.3321	95.55	0.002
tissue*punch	3	0.3872	0.3872	0.1291	0.77	0.511
Error	160	26.7362	26.7362	0.1671		
Total	167	65.9634				

S = 0.408780 R-Sq = 59.47% R-Sq(adj) = 57.69%

x Not an exact F-test.

Table 6.8. Analysis of variance for data set 3 using the reduced model, with interaction.

Analysis of Variance for $\log(F_{peak})$, using Adjusted SS for Tests

Source	DF	Seq SS	Adj SS	Adj MS	F	P
tissue	1	1.2228	0.6926	0.6926	4.16	0.043
punch	3	37.6172	37.6172	12.5391	75.35	0.000
Error	163	27.1234	27.1234	0.1664		
Total	167	65.9634				

S = 0.407923 R-Sq = 58.88% R-Sq(adj) = 57.87%

Table 6.9. Analysis of variance for data set 3 using the reduced model, without interaction.

Punch once again shows significant effect, just as we expected, but here we also see a significant effect of tissue. The larger degree of determination, close to 60%, is most likely caused by the larger span in the punch diameter.

The standard error here is still of the same order as before, being approximately 50%.

As before, the residuals are approximately normally distributed, but not as well as for the other data sets. It is however important to note that without the logarithmic transformation the residuals would be even less normally distributed than they are with the transformation.

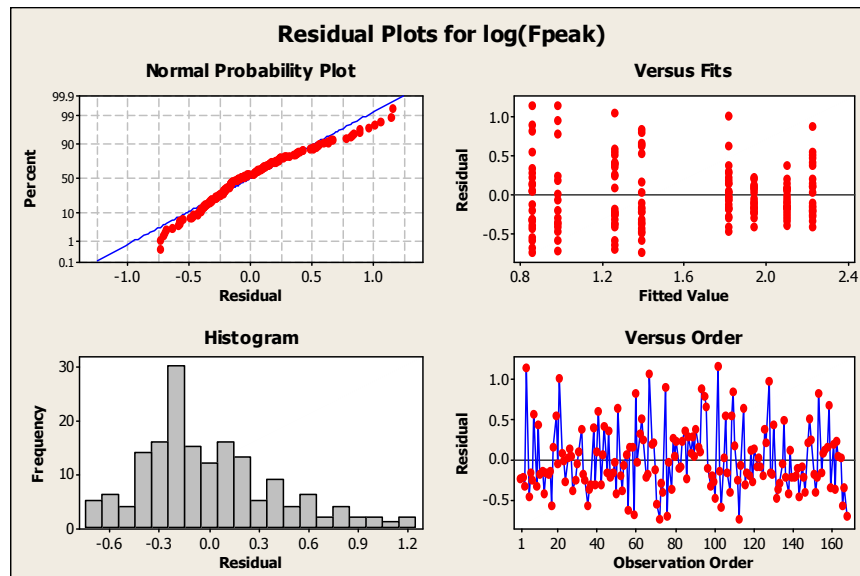


Figure 6.6. Residual plot for data set 3, for the reduced model, without interaction.

The same method was then applied to the force at first damage, with the same result, that there is no effect of round.

6.2.5 Summary and Conclusions

Each tissue was perforated in four test rounds, each round consisting of about 25 perforations, where the entire tissue was covered by each round. Based on the analysis of the randomized tests no significant effect of the test round was found. We conclude that the test rounds do not differ significantly from each other and that it therefore does not matter if the test was randomized between rounds or not. Therefore, in the following the non-randomized test data will be included in the analysis without any correction for tissue aging.

The standard error is approximately 40-50% in these tests, which is quite large and requires a large sample size to show a significant difference between punches that closely resemble each other.

For the helix there seems to be an interaction effect between the tissue and the punch. This will be further investigated in Section 6.3, but with limited data from punches with helix, (see Table 5.1) the possibilities for a more advanced analysis are small.

Observations of residual plots show that the logarithmic transformation results in the residuals being close to normally distributed. This means that the log-normal distribution could be a good approximation for the force distribution of the force measurements. The use of the logarithmic transformation also indicates that when comparing different tissue samples or punches, we should not look at the absolute difference between the force values, rather we should look at the relative difference between them (e.g. by dividing them with each other). This is what we do when we look at absolute differences between the logarithms of force values. In the following, we will present most results on a relative scale, relating the different punches to each other.

6.3 The Effect of the Helix

We have already seen that there is an effect of the helix and that there seems to be an interaction effect with the tissue (see Section 6.2.2). We now want to quantify the effect of the helix and see how this effect varies with different tissue samples. We perform this analysis by comparing individual force values for each combination of tissue sample and punch, and show that the helix in general reduces both the peak perforation force and the force at first damage (Section 6.3.1).

6.3.1 Statistical Analysis

We continue the analysis of the effect of the helix, by including all data where a punch with helix was tested.

Sample ID	Punch Type Size in French			
	Tube		Helix	
	4	6	4	6
P12	25 (0)	25 (0)	24 (1)	24 (0)
P13	49 (1)	-	49 (0)	-
P14	48 (1)	-	47 (3)	-

Table 6.10. Data that allows for a comparison of the effect with and without a helix.

The previous investigation has already shown that there may be an interaction effect between the tissue and the punch with and without a helix. Because of the limited data available for the helix and the interaction effect, the analysis in this case will be limited to just plotting the mean of the logarithm of the force for the different combinations of punch and tissue.

In addition, 95% two-sided error bars have been plotted in the figure. The approximate 95% CI estimated standard error for each average has been calculated as

$$SE_{average} = 1.96 \frac{SE}{\sqrt{n}} \quad (6.5)$$

where n is the number of tests in the average, and SE is the standard error from the analysis of variance. Here we assume it to be 40%, based on the previous analysis in Section 6.2. The number 1.96 comes from the 95% two-sided confidence interval for a normal distribution with known standard deviation. The data has been plotted in Figure 6.7 (peak force) and Figure 6.8 (force at first damage).

In addition, the relative difference in force with and without a helix has been calculated. We will use the data to perform significance testing and since we have four different combinations of punch and tissue, using a simultaneous 95% confidence interval, each individual two-sided confidence interval has to be approximately 99% ($1-p/n$, with $p=0.05$ and $n=4$, using Bonferroni correction).

For the peak force (Figure 6.7), two of the tests groups show a significantly lower force with a helix than without helix at the simultaneous confidence level of 95%. We can see that the data is not completely conclusive as two of the test groups do not show a significant deviation from zero, and so could be identical. However, there is no indication that the helix would increase the perforation force.

For the force at first damage (Figure 6.8), we see that, while the absolute values are significantly lower than for the peak force, the relative differences are very similar. This time the P12RO/6F test also shows a significant difference with and without a helix.

If we wish to have a rule of thumb based on these tests, we could say that using a helix lowers the peak force with 20% on an average.

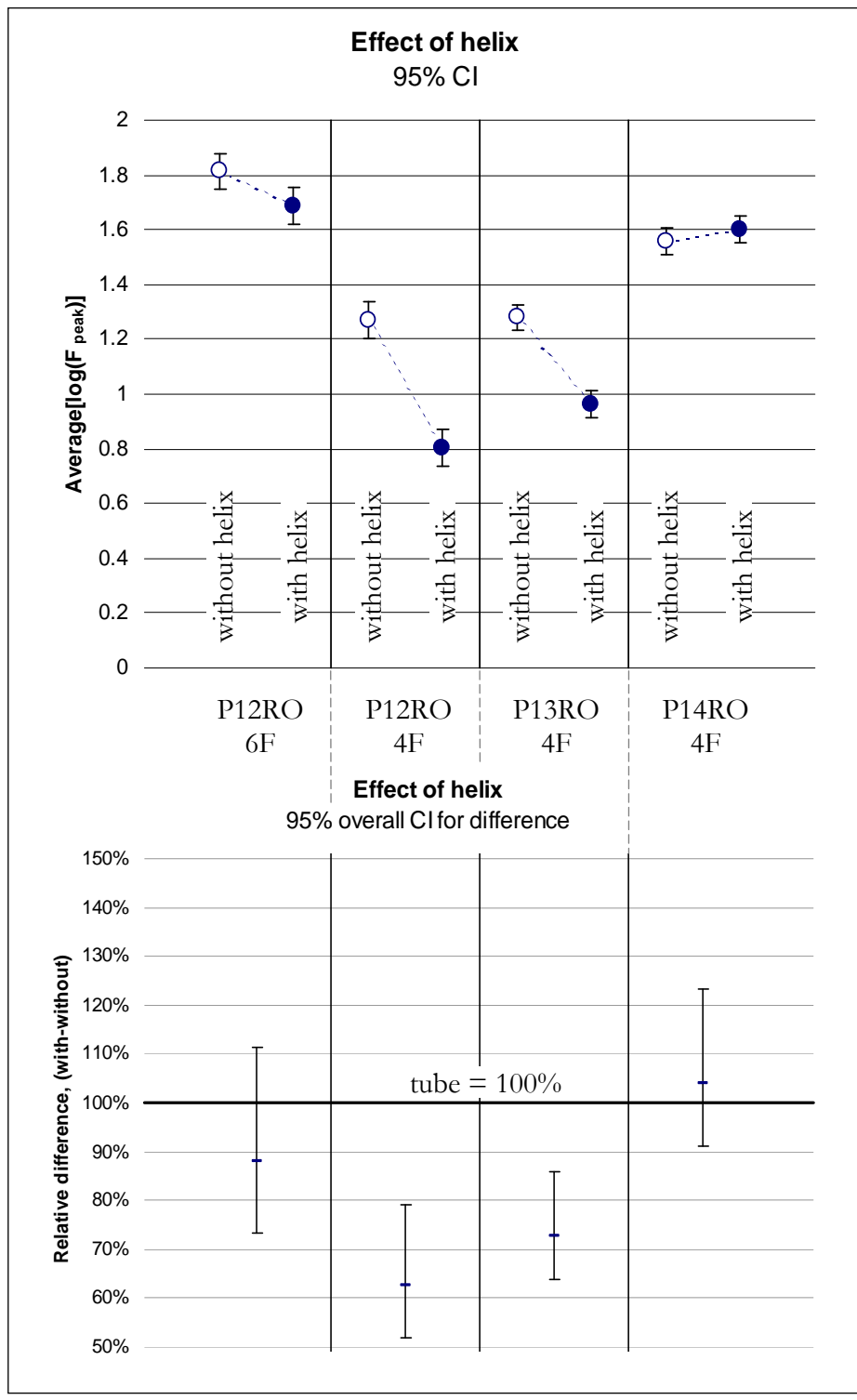


Figure 6.7. Average **peak** force with individual 95% CI (upper chart) and relative difference between force for tubular punch without helix and force for tubular punch with helix with simultaneous 95% CI, so each interval corresponds to approximately 99% (lower chart).

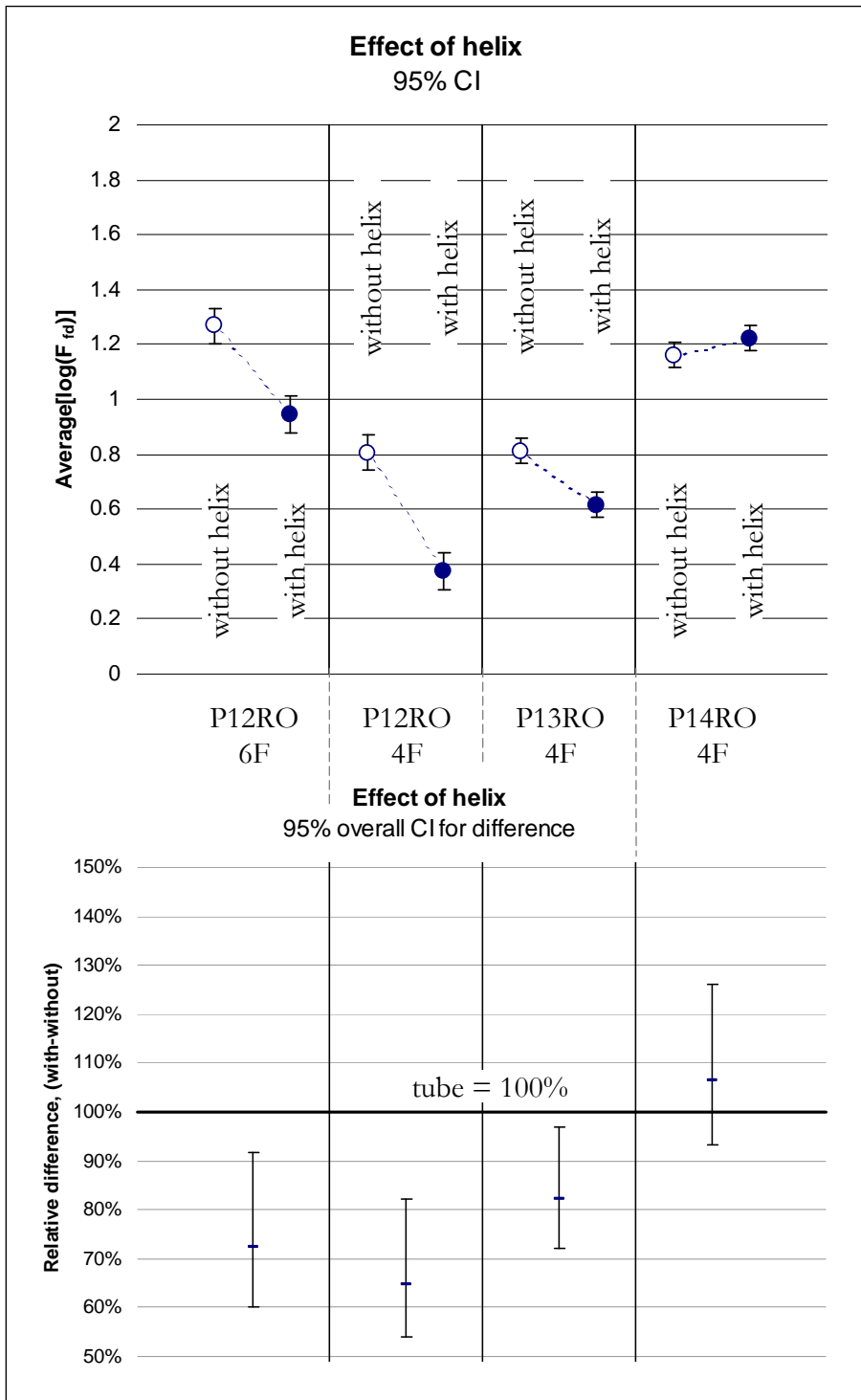


Figure 6.8. Average force at **first damage** with individual 95% CI (upper chart) and relative difference between force for tubular punch without helix and force for tubular punch with helix with simultaneous 95% CI, so each interval corresponds to approximately 99% (lower chart).

6.3.2 Summary and Conclusions

The helix tends to reduce the force by approximately 20% on an average when compared to a tubular punch without a helix. The result is not entirely conclusive, as there seems to be an interaction between tissue and punch, with some tissue samples not showing any effect of the helix. Assuming that the tests were performed identically for the different tissue samples, it could be that the structure or composition of the tissue interacts with how the helix grips the tissue and this in turn could affect if the helix affects the force or not.

The result of this extended analysis is similar to that in [2] where it was concluded that the helix tends to reduce the force, at least for the peak force. Here we see that the same is in fact also true for the force at first damage.

6.4 Statistical Analysis of Solid and Tubular Punches

We now turn to the full analysis that includes a possible effect of punch type and punch diameter. We start by presenting the linear model (Section 6.4.1) and then analyze the data first showing that there are interactions effects between the factors, but that they can be ignored creating a simplified model with only the main effects. The difference between the main effects is plotted graphically (Section 6.4.2). Finally, the relationship between the force and the diameter is investigated, together with a discussion regarding an alternative limiting parameter for the design of the lead tip (Section 6.4.3).

6.4.1 The Linear Model

Similar to the analysis of a possible effect of tissue aging (Section 6.2) we will use the linear model approach for the analysis of the data. Based on the previous findings we will exclude the factor round. We will also exclude all the helix data, since we have seen an interaction between this type of punch and the tissue, and because there is only limited data for that type of punch.

For this analysis, we will also split the factor punch into its two properties, the type (solid or tubular) and the diameter (3, 4, 5, 6, 7 or 8F). We thus still have three factors, and tissue is still the random factor. We will also use the logarithmic transformation of the force data as before (see Section 6.5 for a justification).

The complete statistical model, with interactions, now looks like this:

$$\ln(F_{ijkl}) = \mu + \alpha_i + \beta_j + \gamma_k + (\alpha\beta)_{ij} + (\alpha\gamma)_{ik} + (\beta\gamma)_{jk} + (\alpha\beta\gamma)_{ijk} + \varepsilon_{ijkl} \quad (6.6)$$

The parameters are defined like this⁷:

F_{ijkl}	The force	l is the index for the test within the group defined by a specific tissue, punch and round. The range for l is therefore different for each such combination. Indices should have been used to indicate this, but were omitted because this is obvious from the description of the data set (Table 5.1).
μ	The average of all data.	
ϵ_{ijkl}	The standard error term.	$\epsilon_{ijkl} \sim N(0, \sigma^2)$
α_i	The effect of the tissue, random factor.	$\alpha_i \sim N(0, \sigma_\alpha^2)$
β_j	The effect of the punch type, a systematic factor.	$\sum_j \beta_j = 0$ (only two types so $\beta_1 = -\beta_2$)
γ_k	The effect of the punch diameter, a systematic factor (note that the order is not randomly chosen).	$\sum_k \gamma_k = 0$ $k = 1 \dots 6$ (six different diameters)
$(\alpha\beta)_{ij}$	The interaction between tissue and punch type, a random factor since tissue is a random factor.	$(\alpha\beta)_{ij} \sim N(0, \sigma_{\alpha\beta}^2)$
$(\alpha\gamma)_{ik}$	The interaction between tissue and punch diameter, a random factor since tissue is a random factor.	$(\alpha\gamma)_{ik} \sim N(0, \sigma_{\alpha\gamma}^2)$
$(\beta\gamma)_{jk}$	The interaction between punch type and diameter, a systematic factor.	$\sum_j (\beta\gamma)_{jk} = \sum_k (\beta\gamma)_{jk} = 0$
$(\alpha\beta\gamma)_{ijk}$	The interaction between tissue, punch type and punch diameter; a random factor since the tissue is a random factor.	$(\alpha\beta\gamma)_{ijk} \sim N(0, \sigma_{\alpha\beta\gamma}^2)$

To be able to test for the interactions we inspect the data and find that we can assess all the interaction effects using the following data set:

Data Set	Tissue Samples	Punches	Comment
1	8, 9, 10 and 17	solid and tube 4 and 6F	A nice 2x2 test for the factors punch type and punch diameter.

Table 6.11. The table shows the data set that will be used to test for interaction effects.

⁷ Minitab does not require the sum of random factors over indices of fixed factors to be zero. This does affect some of the F-tests. This has not been further explored in this thesis.

We see that although not being balanced, the data set includes all the different combinations of punch type and diameter listed for each tissue sample, thus forming a complete test matrix with replicates. As before, the fact that the tests are not balanced means that the performed F-tests in some cases will not be exact. Because of the reasonably large sample size for each combination of tissue and punch and because the number of perforations for each combination of tissue and punch are comparable the F-test should still be reasonably accurate and should give a clear indication if an effect is significant or not.

6.4.2 Analysis of the Data

We start the analysis by investigating if there is an interaction effect. Without giving all the details, the procedure is as before. Using Minitab, we use the full model according to equation (6.6) to create an ANOVA table and then remove factors or interaction when they are not statistically significant. During the analysis, we also find four residuals that are too high and we therefore exclude the corresponding data points from the analysis. All of these are from tissue sample P10, which we previously saw has an area with deviating strength. For this analysis of the possible interactions, we also accept the removal of a single data point with a very high negative residual. The resulting analysis is shown in Table 6.12 and Table 6.13.

The analysis shows that there are statistically significant interaction effects. For completeness, we should build a model where some interactions are included. However, we can also see that the interaction effects are smaller than the main effects, so maybe we can exclude them. As a test, we perform the same analysis without the interactions to see what happens to the value of R^2 . The resulting analysis is shown in Table 6.14 and Table 6.15.

Analysis of Variance for $\log(\text{Fpeak})$, using Adjusted SS for Tests

Source	DF	Seq SS	Adj SS	Adj MS	F	P
p_{type}	1	1.4837	1.7230	1.7230	14.43	0.000
p_{diam}	1	24.3486	23.3088	23.3088	117.10	0.002 x
t_{issue}	3	9.2604	9.3662	3.1221	15.68	0.024
p_{type}*p_{diam}	1	0.4000	0.4251	0.4251	3.56	0.060
p _{diam} *t _{issue}	3	0.5972	0.5972	0.1991	1.67	0.174
Error	372	44.4158	44.4158	0.1194		
Total	381	80.5057				

S = 0.345539 R-Sq = 44.83% R-Sq(adj) = 43.49%

x Not an exact F-test.

Table 6.12: Analysis of variance for the **peak** force, using a reduced model. We have retained the interaction between punch diameter and tissue, although it is not significant, for comparison with the force at first damage, where it is significant.

Analysis of Variance for log(Ffd) using Adjusted SS for Tests

Source	DF	Seq SS	Adj SS	Adj MS	F	P
ptype	1	4.6773	5.2268	5.2268	52.71	0.000
pdiam	1	32.5551	31.1218	31.1218	76.21	0.003 x
tissue	3	10.6866	10.9527	3.6509	8.94	0.053
ptype*pdiam	1	1.1930	1.2523	1.2523	12.63	0.000
pdiam*tissue	3	1.2253	1.2253	0.4084	4.12	0.007
Error	372	36.8901	36.8901	0.0992		
Total	381	87.2275				

S = 0.314908 R-Sq = 57.71% R-Sq(adj) = 56.68%

x Not an exact F-test.

Table 6.13: Analysis of variance for the force at **first damage**, using a reduced model. We can see that some of the interaction effects are significant. However, we can also see that the mean sum of squares is smallest for the two interaction effects.

Analysis of Variance for log(Fpeak), using Adjusted SS for Tests

Source	DF	Seq SS	Adj SS	Adj MS	F	P
ptype	1	1.4837	1.6735	1.6735	13.86	0.000
pdiam	1	24.3486	23.4952	23.4952	194.53	0.000
tissue	3	9.2604	9.2604	3.0868	25.56	0.000
Error	376	45.4131	45.4131	0.1208		
Total	381	80.5057				

S = 0.347533 R-Sq = 43.59% R-Sq(adj) = 42.84%

Table 6.14: Analysis of variance for the **peak** force, ignoring the interactions.

Analysis of Variance for log(Ffd), using Adjusted SS for Tests

Source	DF	Seq SS	Adj SS	Adj MS	F	P
ptype	1	4.6773	5.0842	5.0842	48.63	0.000
pdiam	1	32.5551	31.4474	31.4474	300.81	0.000
tissue	3	10.6866	10.6866	3.5622	34.07	0.000
Error	376	39.3084	39.3084	0.1045		
Total	381	87.2275				

S = 0.323332 R-Sq = 54.94% R-Sq(adj) = 54.34%

Table 6.15: Analysis of variance for the force at **first damage**, ignoring the interactions.

We can see that the R^2 values are only slightly reduced by the exclusion of the interactions. Here we are not interested in any minor effects of the interactions and also in order to work with a simple model we will ignore the interactions in the full analysis of the data. This also allows us to use all the available test data. However, we chose to exclude the helix data, since this analysis was already completed in Section 6.3. Because there is some weak interaction between the factors, the analysis will be approximate. The result of the analysis is shown in Table 6.16 and Table 6.17 with the corresponding residual plots in Figure 6.9 and Figure 6.10.

Analysis of Variance for $\log(F_{\text{peak}})$, using Adjusted SS for Tests

Source	DF	Seq SS	Adj SS	Adj MS	F	P
ptype	1	0.004	3.200	3.200	24.67	0.000
pdiam	5	152.416	130.326	26.065	200.99	0.000
tissue	13	39.954	39.954	3.073	23.70	0.000
Error	1157	150.047	150.047	0.130		
Total	1176	342.422				

S = 0.360120 R-Sq = 56.18% R-Sq(adj) = **55.46%**

Variance Components, using Adjusted SS

Source	Estimated Value
tissue	0.03880
Error	0.12969

Least Squares Means for $\log(F_{\text{peak}})$

ptype	Mean
tube	1.925
solid	1.770
pdiam	
3	1.178
4	1.515
5	1.921
6	2.000
7	2.085
8	2.385

Table 6.16: Result of analysis of variance for the **peak** force, using all data (except helix). Variance terms and least square means have been included for further processing. No data points have been excluded for this analysis.

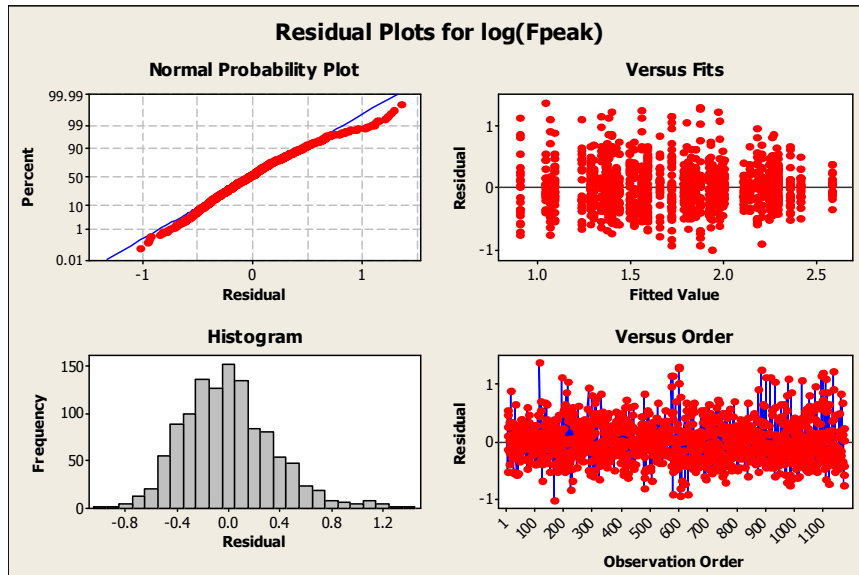


Figure 6.9. Residual plot for the **peak** force, all data (except helix). A deviation from normal residuals can be seen at the high end indicating a longer tail at the high end. In addition, in the residuals versus observation order it can be seen that extreme residuals tend to belong to specific pieces of tissue.

Analysis of Variance for log(Ffd), using Adjusted SS for Tests

Source	DF	Seq SS	Adj SS	Adj MS	F	P
ptype	1	2.514	9.999	9.999	79.23	0.000
pdiam	5	156.662	142.381	28.476	225.63	0.000
tissue	13	36.808	36.808	2.831	22.43	0.000
Error	1154	145.641	145.641	0.126		
Total	1173	341.625				

S = 0.355254 R-Sq = 57.37% R-Sq(adj) = **56.67%**

Variance Components, using Adjusted SS

Source	Estimated Value
tissue	0.03576
Error	0.12621

Least Squares Means for log(Ffd)

ptype	Mean
tube	1.4324
solid	1.1593
pdiam	
3	0.6483
4	0.9650
5	1.2337
6	1.5155
7	1.5405
8	1.8723

Table 6.17: Result of analysis of variance for the force at **first damage**, using all data (except helix). Variance terms and least square means have been included for further processing. Three data points have been excluded for this analysis.

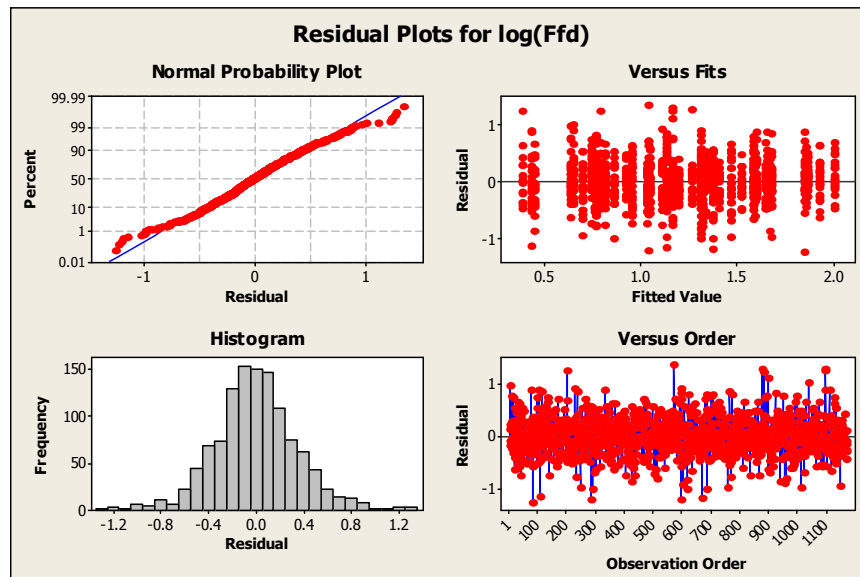


Figure 6.10. Residual plot for the force at **first damage**, all data (except helix). A deviation from normal residuals can be seen at the high and low end indicating a wider distribution than the normal distribution.

We see that the standard error is still approximately 40% [$e^{0.35}=1.40$]. This is in line with the previous results from Sections 6.2 and 6.3, where 40% was used as a “default” standard error.

We can also see that the variance for the logarithm of the peak force is approximately the same as the variance for the logarithm of the force at first damage. This indicates that the **relative** error is the same for both the peak force and the force at first damage.

The variation between tissue samples seems to correspond to about 20% and the standard error to about 80% of the total variance. This means that the variation within a single tissue sample is larger than the variation between different tissue samples. Note that this conclusion is only valid for porcine tissue from healthy pigs as the ones used in this test.

Since this is not a balanced test design estimating the error terms exactly is not possible, but we will use an approximation. First, we will plot the least square means for the punch diameter, ignoring the effect of punch type. The approximate **individual** 95% confidence intervals are calculated using the following error term for the means:

$$SE_{mean} = 1.96 \sqrt{\frac{\sigma^2}{n} + \frac{\sigma_\alpha^2}{m}} \quad (6.7)$$

The variance terms are as defined in the statistical model (6.6) and can be found in the results of the analysis (Table 6.16 and Table 6.17), n is the number of data points for the specific diameter, and m is the number of tissue samples for the specific diameter.

We plot the least square means for the individual diameters in Figure 6.11 and the least square means for the tubular and solid punches in Figure 6.12.

As can be seen the force is lower for the solid punch, a little surprising as it can be assumed that the “force” should be higher for the tubular punch and that it should therefore go through the tissue easier. This is not the case, indicating that the shape of the tip is important and that the outer diameter is not the only contributing factor. We can also calculate the difference between the two punches. We now need to combine the two error terms for the two punch types. Since these two punches have been tested on largely the same tissue samples, we will assume that we can ignore the tissue part of the error. The result is shown in Figure 6.13.

We see that the peak perforation force is about 15% lower and the force at first damage about 25% lower for the solid punch compared to the tubular. The result is statistically significant and is surprising when thinking about the contact area between the punch and the tissue and also considering the sharper edges on the tubular punch. It is clear that the contacting surface area is not the only important factor, but that the actual shape of the punch is important.

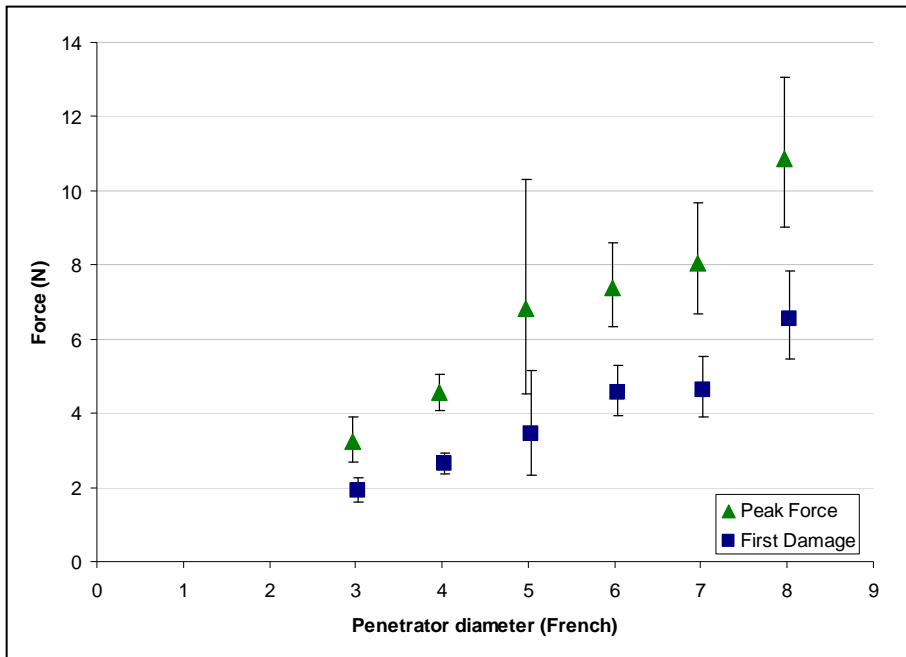


Figure 6.11: Least square means of the force for the punch diameter with approximate **individual** 95% confidence intervals. Note that these are the individual confidence intervals, and cannot be used directly to compare different data points, since the different points are partly correlated. For instance, some of the points originate from almost the same tissue samples, while others come mainly from different tissue samples. The large uncertainty for the diameter 5F punch is because this data comes from only one tissue sample. The increasing errors towards higher diameters/levels of force come from the logarithmic transformation. The errors are (approximately) equal for the mean of the logarithmic data, and so become unequal when the data is transformed back to linear scale.

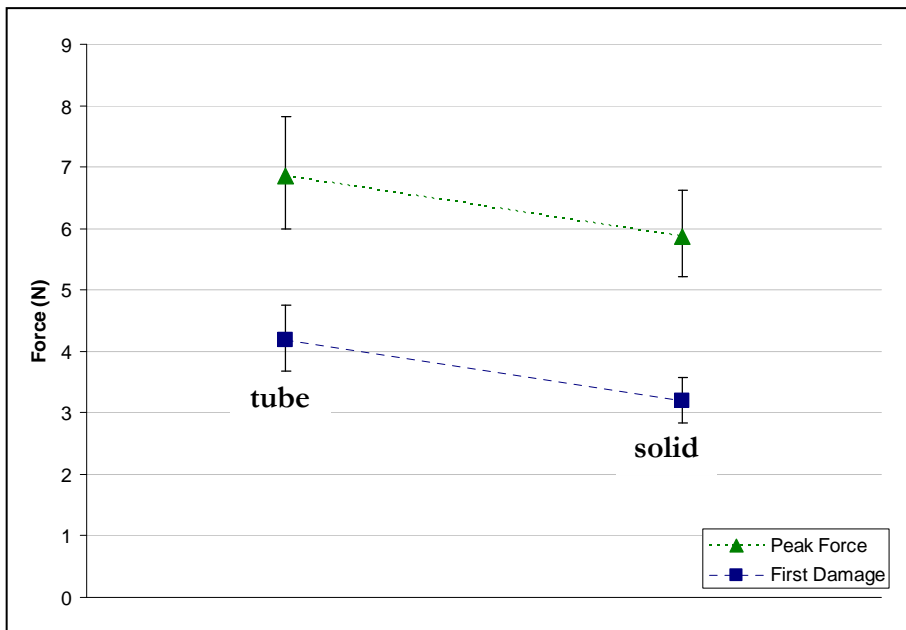


Figure 6.12: Mean force for the two different punches, with approximate **individual** 95% confidence intervals.

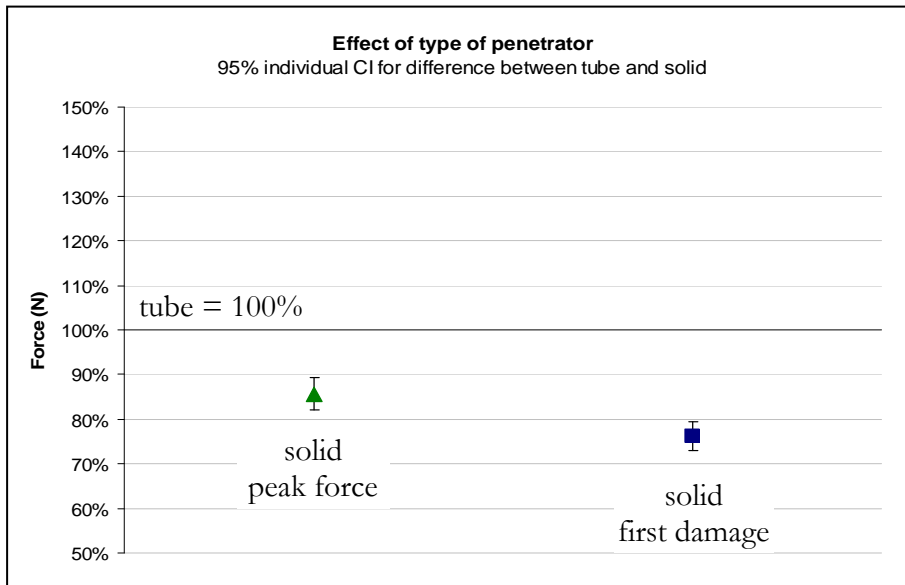


Figure 6.13: Difference between tubular and solid punches. Here the effect of tissue has been ignored.

6.4.3 Force as a Function of the Diameter

We now return to how the force depends on the diameter. From Figure 6.11 we see something that looks like a linear relationship between the force and the diameter. Performing a statistically correct linear regression on these data would have to take into account the different confidence interval for the different diameters. However, it gets even more complicated as the force values for the different data points are correlated (as described in the figure text). To simplify the calculations we will ignore the difference in confidence interval and perform an un-weighted linear regression as shown in Figure 6.14.

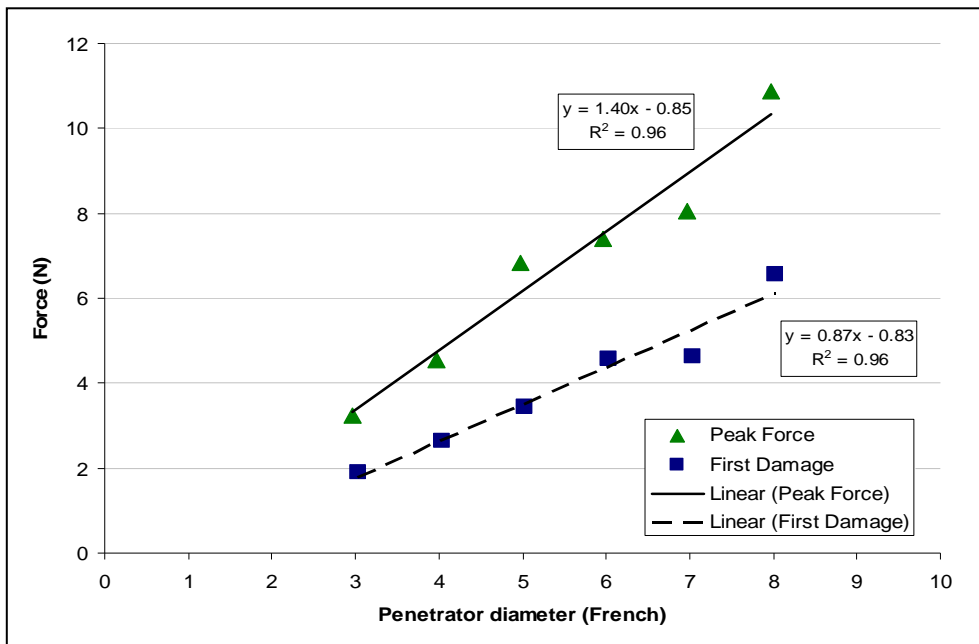


Figure 6.14: Linear fit for the force for different punch diameters. There is nothing in this fit that indicates that a non-linear relationship would be more appropriate.

Sometimes the tip pressure is used as a limiting parameter in the design of leads. Here the tip pressure is usually defined as the force divided by the area of the lead tip (calculated using the “projected” outer diameter). The perforation forces in Figure 6.14 can be recalculated to a pressure using the outer diameter of the punches. The same can be done for the fitted lines. Often the area of the lead tip has been considered as a more important parameter than the diameter, so we perform the plotting of the pressure versus the punch area in Figure 6.15.

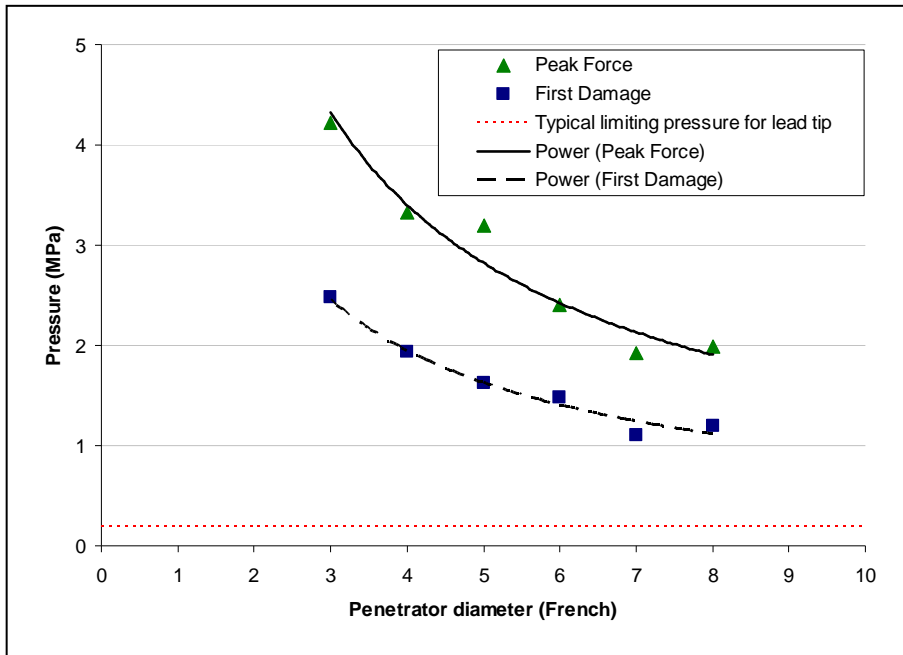


Figure 6.15: Punch pressure as a function of punch tip area. The chart shows the pressure when the punch perforates the tissue and the power-fit lines serve the same purpose as the linear-fit lines in Figure 6.14. The dashed horizontal line at the bottom of the chart shows the typical limiting pressure during lead design. The lead is designed to bend at forces exceeding this pressure. As can be seen there is a margin to the “mean” pressure levels measured for the porcine cardiac tissue. However in order to assess the risk of perforation the actual distribution of real cardiac tissue must be taken into account together with the actual distribution of the stress applied during implantation and within a few weeks of implantation.

As can be seen from the figure the pressure is **not** constant with the diameter. Rather the pressure decreases with the diameter. Therefore, the pressure may not be a good limiting parameter, as it should be adjusted for each lead tip diameter. Figure 6.16 instead shows the perforation force divided with the diameter. As can be seen this new parameter is much less dependent on the diameter than the force itself or the pressure. It may be that the quotient between tip force and tip diameter would be a better limiting parameter than a pressure value. However, this needs to be investigated further as this analysis has been for the “mean” force only and the perforations in real life occur as combination of the strength distribution of actual cardiac tissue with the stress distribution of real leads.

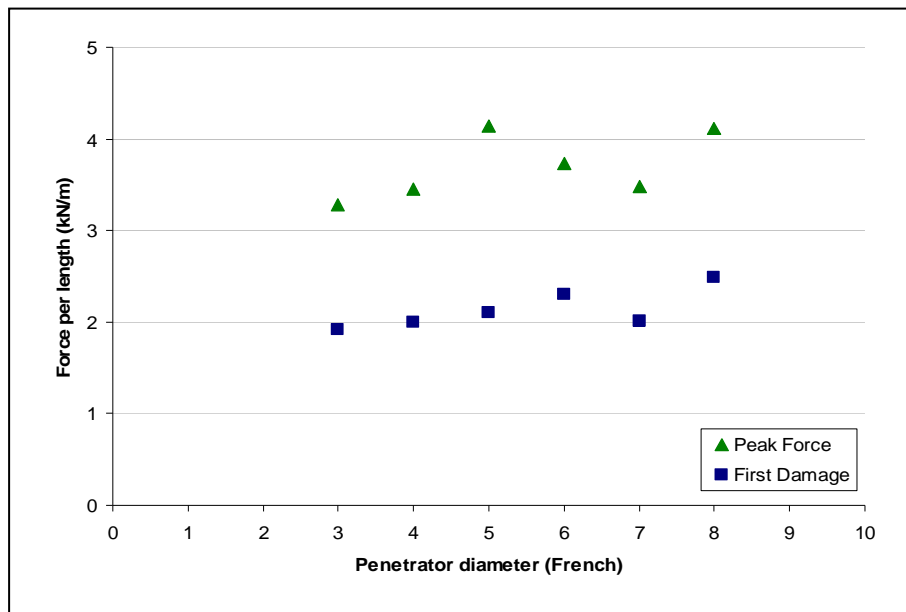


Figure 6.16: The quotient between the force (in N) and the diameter (in mm) as a function of diameter. It can be seen that this quotient is almost constant over this range of punch diameters.

6.4.4 Summary and Conclusions

This section describes the analysis of variance for all of the perforation data, excluding only the helix data that was analyzed earlier (see Section 6.3).

The analysis starts by showing that there are interaction effects between the three factors punch type (solid or tubular) the punch diameter and the tissue. However, it is also shown that this effect is small compared to the main effects, and the effect is therefore dropped from the remaining analysis. This allows for an ANOVA analysis of the complete data set with only the main effects present.

From this analysis, several things can be concluded:

- The force at first damage is about 40% lower than the peak force (Figure 6.11). This is not surprising as the force at first damage by definition must always be lower than, or possibly equal to, the peak force. More interesting is that the overall behavior of the force at first damage behaves qualitatively in the same way as the peak force.
- The solid punch shows a lower perforation force than the tubular punch. This is surprising since they have the same outer area and the first thought would lead one to believe that the sharper outer edge of the tube would cut more easily through the tissue. The failure modes of soft biological tissue are discussed in [1] (mode-I and mode-II failures) and this may be part of the explanation for the higher force for the tubular punch. The mode-I failure mode is a “splitting” failure mode while mode-II is a cutting failure mode. Maybe the sharper edge grips the tissue and increases the forces needed for the splitting mode-I failure mode, while not being sharp enough to create the mode-II failure mode.

- The perforation force is approximately a linear function of punch diameter. Section 6.4.3 discusses the usefulness of using a fixed pressure as a limiting parameter for lead tip design and proposes that the quotient between the force and the diameter might be a better choice. This quotient does **not** depend strongly on the diameter and therefore a single limiting value could be used for different diameters. The pressure on the other hand does depend on the diameter, with lower forces for larger diameters (see also [1] for similar results).

6.5 Discussion Regarding the Logarithmic Transformation

6.5.1 Introduction

In this report, the logarithmic transformation has been used for the force data. In this section, the usefulness of a transformation is discussed (Section 6.5.2) and a justification for the logarithmic transformation is presented (Section 6.5.3).

6.5.2 Why a Transformation at all?

When applying the linear model we assume that the data (or rather the residuals) are normally distributed. However, for the force measurements we know that it is not possible to measure a negative force so the idea of normally distributed residuals can only be an approximation. If the standard deviation of the residuals were small, the normal distribution would be a good approximation as the probability would be very small of large negative residuals. However, in this case the relative standard error is about 40% (see Section 6.4.2) so the normal distribution is no longer a good approximation.

Another reason for some kind of transformation is the observation that there seems to be many “deviating” high force values. This can be an indication of outliers, but it can also be an indication that the normal distribution is not the best choice. This can also be illustrated by performing the full analysis of Section 6.4, but without the logarithmic transformation. Here we will only look at the residuals.

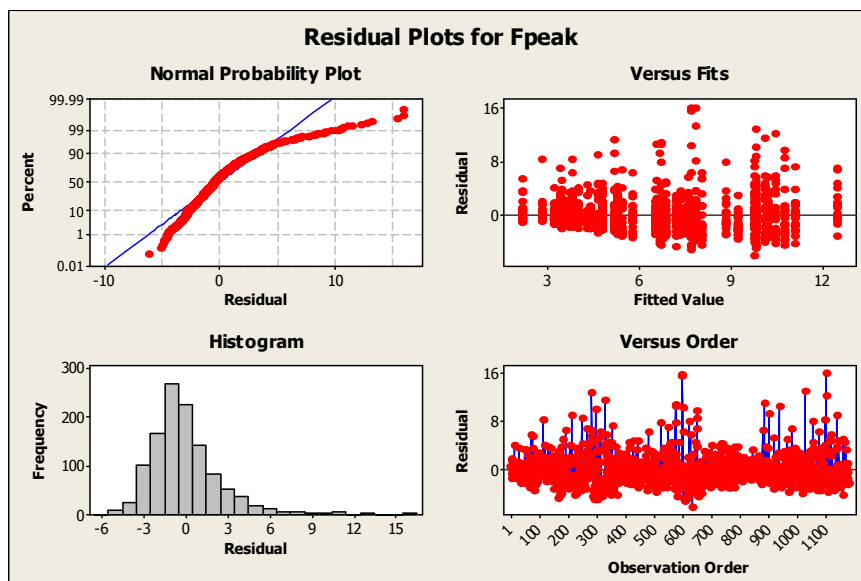


Figure 6.17: Residuals for the peak force and the force at first damage, without the logarithmic transformation of the force.

We observe several things in these graphs:

- The curve in the normal probability plot is far from normal.
- The variance of the residuals looks larger for larger fitted values.
- The lower two figures indicate a large number of potential “outliers” for large positive residuals.

Finally, one might expect that tougher tissue samples (higher perforation force) will also exhibit a higher standard deviation. As a first approach, one could assume that the standard deviation is directly proportional to the average perforation force.

All of these observations lead us towards the need for some type of transformation of the original data before we can perform any statistical analysis of the data.

6.5.3 Choosing the transformation

One often used distribution function is the log-normal distribution [5]. It has the property of only being defined for positive values of the random variable and it allows for a long tail towards higher values. It can be modeled to resemble a normal distribution by choosing a small dispersion (corresponding to the standard deviation for the normal distribution).

In simple terms, if we have a variable X and the logarithm of X is normally distributed, then we say that X is log-normally distributed.

In our case, we have indications that this could be a good transformation. One of the most important indications is that taking the logarithm transforms the increasing variance of the residual into a constant variance, by the properties of the logarithm; e.g. $\log(a/b) = \log(a) - \log(b)$.

We can test this by performing the same analysis as in Figure 6.17 once more, but this time with the logarithmic transformation. In fact we have already done this in Section 6.4.2 already, see Figure 6.9. Inspection of this figure shows that:

- The normal distribution plot now shows a much better fit.
- The dependence of the variance of the residuals on the fitted value is reduced.
- The number of positive potential outliers is reduced.

There are still deviations from the normal distribution, but mainly for high perforation force values. Since we are mainly interested in the lower force values, the log-normal distribution would be a good first choice for the distribution of the perforation force. The same conclusion is valid for both the peak force and for the force at first damage.

This justifies the use of the logarithmic transformation throughout this thesis.

6.5.4 Summary and Conclusions

We show that the log-normal distribution is a good first choice as an approximation for the distribution of the collected force data, both for the peak force and for the force at first damage. This distribution has the properties that we expect from the force distribution, one of them being that the random variable is limited to positive numbers. By inspecting the residuals we also see that the logarithmic transformation results in close to normally

distributed residuals with only very little dependence on the fitted variable. This justifies the use of the logarithmic transformation throughout this thesis.

7 Summary and Conclusions

In this chapter, we start by answering the key questions from Chapter 3 (Section 7.1), we continue with emphasizing the most important findings in the thesis (Section 7.2) and finish by giving recommendations for possible future work (Section 7.3).

7.1 Answers to Key Questions

We now revisit our original key questions from Section 3 to see if we have managed to answer all of them.

No	Question	Answer
Q1	Is there a difference in force between different punches?	<p>There is a difference between the different punches, with the main results being:</p> <ul style="list-style-type: none"> • The helix tends to reduce the perforation force, but does show an interaction with the tissue. The average reduction in perforation force is estimated to be 20% compared to the tubular punch (Section 6.3.1). • The solid perforator shows a 15% (peak) and 25% (first damage) lower force than the tubular punch (Section 6.4.2). • The relationship between perforation force and diameter seems linear. This is surprising since often the lead tip pressure is used to characterize the lead instead of the force, and the pressure does not show a linear relationship with the diameter, nor with the tip area. In fact, the pressure required to perforate the tissue decreases as the diameter increases (Section 6.4.3). Results from [1] provide insight to why this is the case and is probably related to the properties of crack formation in the ventricular tissue. • From this analysis, it is also shown that the quotient between the force and the diameter might be a better parameter than the pressure (Section 6.4.3).
Q2	What is the statistical distribution for the measured force values?	<p>The analysis shows that the log-normal distribution can be used to model the force data. This is valid for both the peak force and the force at first damage (Section 6.5). Therefore throughout the thesis the force was transformed using the logarithm before being analyzed using e.g. ANOVA.</p>
Q3	Is the tissue homogeneous?	<p>The tissue is heterogeneous. Specifically at least one tissue sample was shown to have an area that was stronger than other parts of the tissue, but also the tissue samples as a group show heterogeneous properties. The peak force shows a stronger heterogeneity than does the force at first damage. The analysis also resulted in the definition of a correlation coefficient that can be used to characterize the tissue in terms of how homogeneous or heterogeneous it is (Section 6.1).</p>

No	Question	Answer
Q4	Are different pieces of porcine tissue "equal"?	Different porcine tissue samples are not equal. It was seen in the investigation of the homogeneity of the tissue samples that some of them stand out from the others (Section 6.1). Of the total variance, the contribution from the tissue samples is about 20%. This means that the variation within a tissue sample is still larger than between the different tissue samples (Section 6.4.2). Because the correlation coefficient defined is so different for different tissue samples, one should not rely on the results from testing on only a single piece of tissue.
Q5	Does the tissue age during the test?	No indication of tissue aging was found in the analysis (Section 6.2). This allows the use of test data that was not fully randomized in terms of order of the punches.

Table 7.1. The table summarizes the answers to the key questions from Section 3.

7.2 Final Conclusions

Finally, we summarize the most important conclusions of this thesis:

- The tissue does not age during testing, so randomizing the order of the perforations is not required (although it may be recommended).
- The tissue is not homogeneous, but has stronger and weaker areas. This means that one should not rely on tests performed on a single piece of tissue for more general conclusions. This work also leads to the definition of a correlation coefficient that can be used to characterize the level of homogeneity of the tissue. It is important to note that since the tissue is not homogeneous there is also a correlation between perforations performed in proximity to each other. This means that the requirement of different measurements being independent in the linear model is not fulfilled. This intrinsic tissue variation becomes part of the residual error term in the linear model, when not taken care of in any other way.
- The log-normal distribution can be used to model the perforation force data. This implies that the average and the standard deviation of the force data should not be used, since they will be biased by the skewed distribution. This finding has implications on other perforation tests being performed where it has not been shown that the gathered data is normally distributed.
- The perforation force is approximately linearly proportional to the diameter. Actually, the quotient between the force and the diameter is close to being a fixed number that does not depend on the diameter. This could be a better definition for a limiting value for the lead tip than is the lead tip pressure, which is sometimes used as a characteristic.

7.3 Recommendations for Future Work

This thesis was based on porcine tissue from presumably healthy pigs. Continued work that relates these results with those for a much more diversified human heart patient population is needed. This work could be both of a practical nature (perforation tests and other mechanical test) or analytical (building a statistical model based on already available knowledge).

For future testing, it is recommended to create balanced test designs. Such a design of experiments will allow for easier analysis of the data including the possible interactions between factors. Such testing should also investigate what the best balance between number of tested tissue samples and the number of perforations per tissue sample is. With the variation seen between tissue samples it could be beneficial to increase the number of tissue samples. Such tests could also include mapping the strength for different parts of the heart, for instance comparing the septum with the apex and with the outer ventricular wall. The key question could be if these are identical in terms of perforation force.

The effect of the shape of the tip should be more carefully investigated. For instance, does the “sharpness” of the edge of the punch affect the perforation force? Does a more rounded tip shape (like for passive leads) increase or decrease the perforation force? From these tests, the author would guess that it would decrease the force, but this would have to be investigated.

In addition, the test method itself should be analyzed to see how it compares with perforations in a real heart. In this test equipment the backing plate, specifically the size of the holes in it, can be expected to affect the perforation force. This is especially valid for the peak perforation force, while the force at first damage might be less affected by it, since this initial perforation occurs when the perforator still has some distance to go to the bottom plate.

Finally, other statistical tests are still possible to perform on this data set. An example would be to compare the distribution of the force at first damage with a force at a random position during the passage through the myocardium. This would give an indication if the endocardium or the tissue close to the endocardium is stronger or weaker than the average strength of the myocardium tissue.

References

- [1] Gasser, C., Gudmundson, P. & Dohr, G. (2009): *Failure mechanisms of ventricular tissue due to deep penetration*. Journal of Biomechanics, Volume 42, Issue 5, Pages 626-633.
- [2] Hosselton, R. (2008): *Experimental Heart Wall Penetration*. Master's Degree Project. Department of Solid Mechanics, Royal Institute of Technology, Stockholm, Sweden.
- [3] Lindgren, A. & Jansson, S. (1992): *Heart Physiology and Stimulation*. Siemens-Elema AB, Solna, Sweden.
- [4] Tamhane, A. C., Dunlop, D. D. (2000): *Statistics and Data Analysis from Elementary to Intermediate*. Prentice-Hall.
- [5] Levin, D. M. (2001): *Applied statistics for engineers and scientists*. Prentice-Hall.